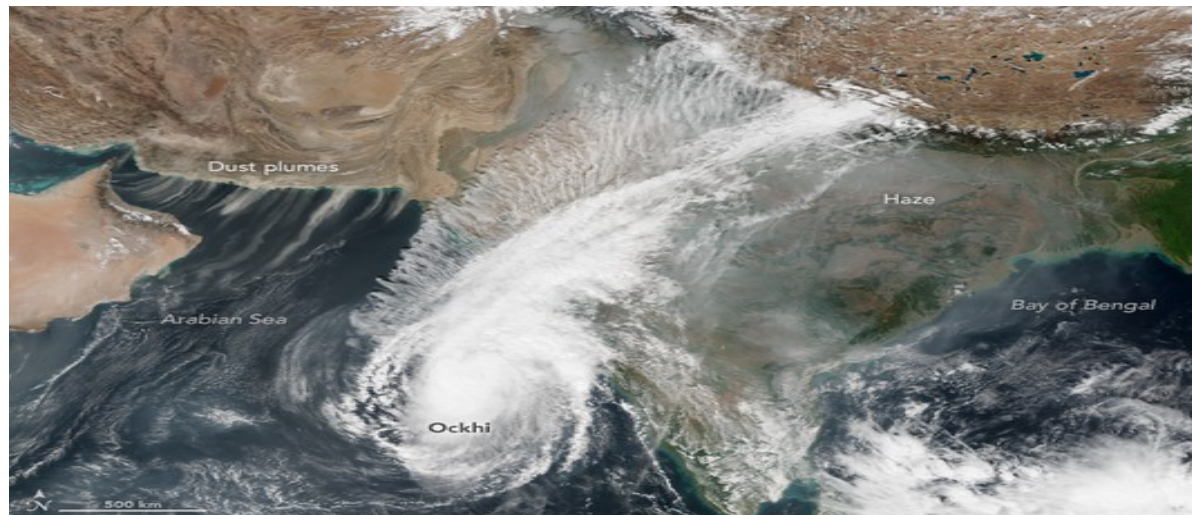


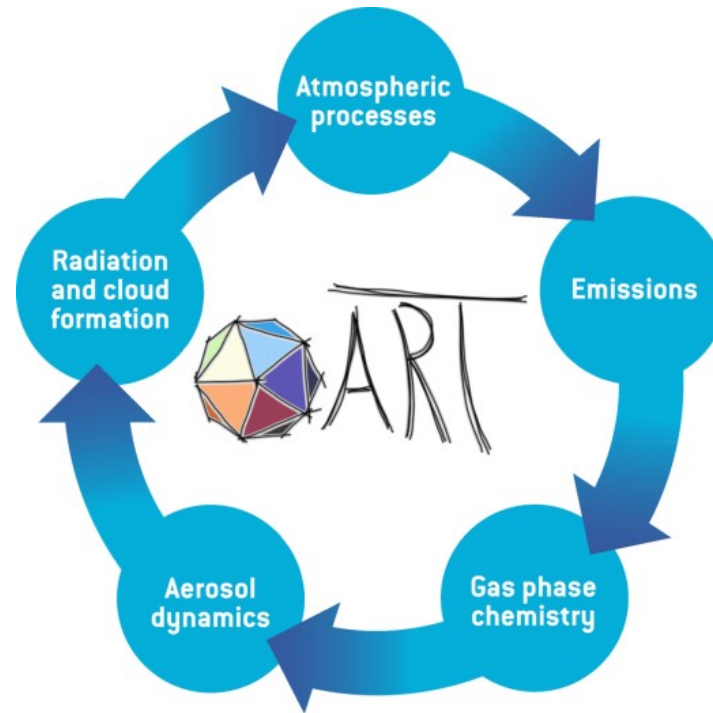
Status of COSMO-ART & ICON-ART

Heike Vogel

Institute of Meteorology and Climate Research, KIT, Karlsruhe



Development and applications of ICON-ART



Implementation of a point source

At a given point:

```
<pntSrc id="RNDFACTORY">  
  <lon type="real">2.351667</lon>  
  <lat type="real">48.856667</lat>  
  <substance type="char">testtr</substance>  
  <source_strength type="real">1.0</source_strength>  
  <height type="real">150.</height>  
  <unit type="char">kg s-1</unit>  
  <startTime type="char">2014-03-29T00:00:00</startTime>  
  <endTime type="char">2014-03-29T01:00:00</endTime>  
</pntSrc>
```

Uniform emission profile:

Between surface and given height

```
<pntSrc id="Eyjafjalla">  
  <lon type="real">-19.36</lon>  
  <lat type="real">63.63</lat>  
  <substance type="char">testtr</substance>  
  <source_strength type="real">1.0</source_strength>  
  <height type="real">-6000.</height>  
  <unit type="char">kg s-1</unit>  
  <startTime type="char">2014-03-29T04:00:00</startTime>  
  <endTime type="char">2014-03-29T05:00:00</endTime>  
</pntSrc>
```

Between given height_bot and height

```
<pntSrc id="Hekla">  
  <lon type="real">-19.4</lon>  
  <lat type="real">63.59</lat>  
  <substance type="char">testtr</substance>  
  <source_strength type="real">1.0</source_strength>  
  <height type="real">5000.</height>  
  <height_bot type="real">1491.</height_bot>  
  <unit type="char">kg s-1</unit>  
  <startTime type="char">2014-03-29T00:00:00</startTime>  
  <endTime type="char">2014-03-29T01:00:00</endTime>
```

Implementation of a point source

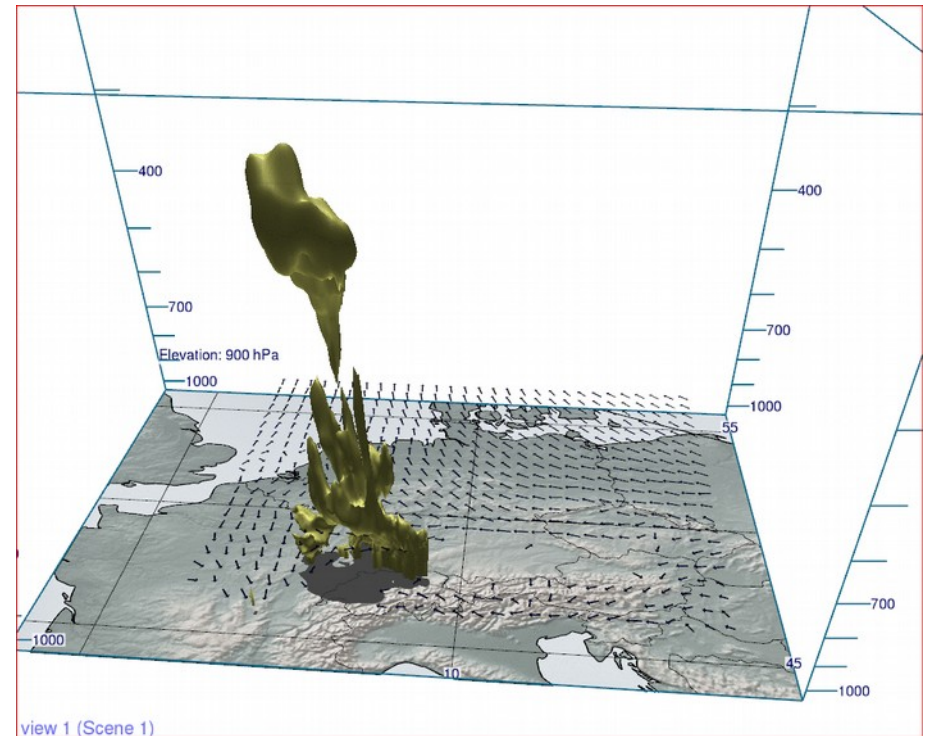
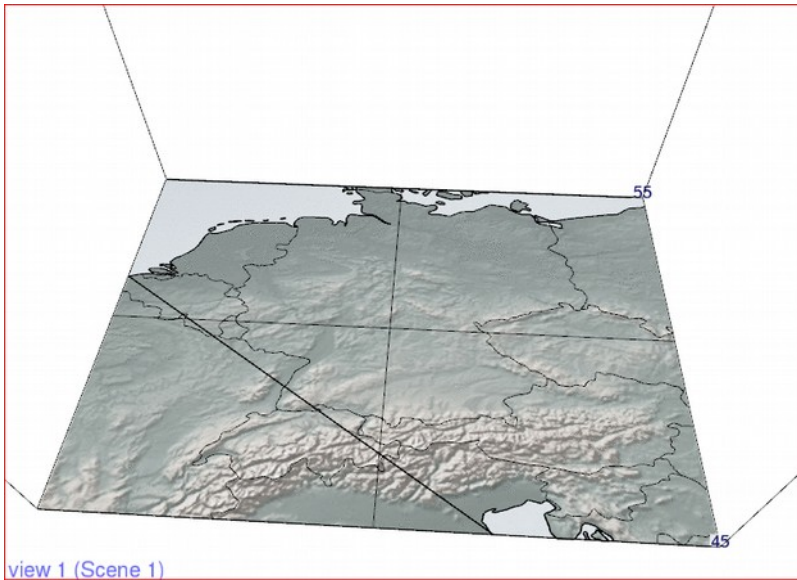
Emission profile:

File Edit View Bookmarks Settings Help

```
!DOCTYPE tracers SYSTEM "sources_selTrnsp.dtd">
```

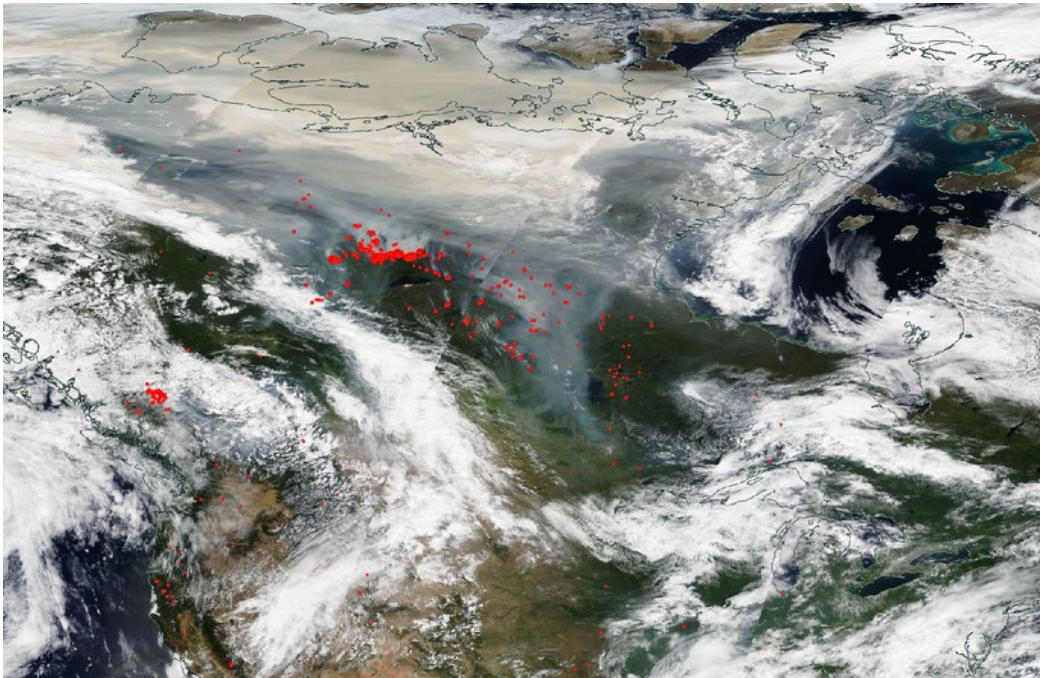
```
<sources>
  <pntSrc id="Eyjaf1">
    <lon type="real">-19.62</lon>
    <lat type="real">63.63</lat>
    <substance type="char">ash_insol_acc</substance>
    <source_strength type="real">500.0</source_strength>
    <height type="real">9000.</height>
    <height_bot type="real">1666.</height_bot>
    <emiss_profile type="char">0.0076 * [z_star] - 0.5 * sqrt(pi) * 0.9724 * 0.3078
      * erf((0.4481 - [z_star]) / 0.3078) / 0.524647415</emiss_profile>
    <unit type="char">kg s-1</unit>
    <startTime type="char">2010-04-03T00:00:00</startTime>
    <endTime type="char">2014-04-31T00:00:00</endTime>
  </pntSrc>
  <pntSrc id="Eyjaf2">
    <lon type="real">-19.62</lon>
    <lat type="real">63.63</lat>
    <substance type="char">ash_insol_coa</substance>
    <source_strength type="real">500.0</source_strength>
    <height type="real">-4000.</height>
    <emiss_profile type="char">0.5 / (4 * pi) * cos(2 * pi * [z_star] / 0.5) + [z_star]</emiss_profile>
    <unit type="char">kg s-1</unit>
    <startTime type="char">2010-04-03T00:00:00</startTime>
    <endTime type="char">2014-04-31T00:00:00</endTime>
  </pntSrc>
```

Examples for a point source

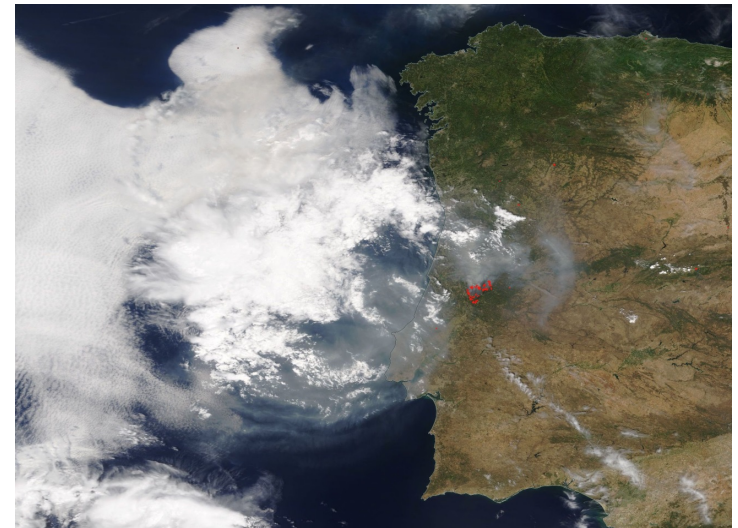


Implementation of vegetation fire emissions

Canada 2017

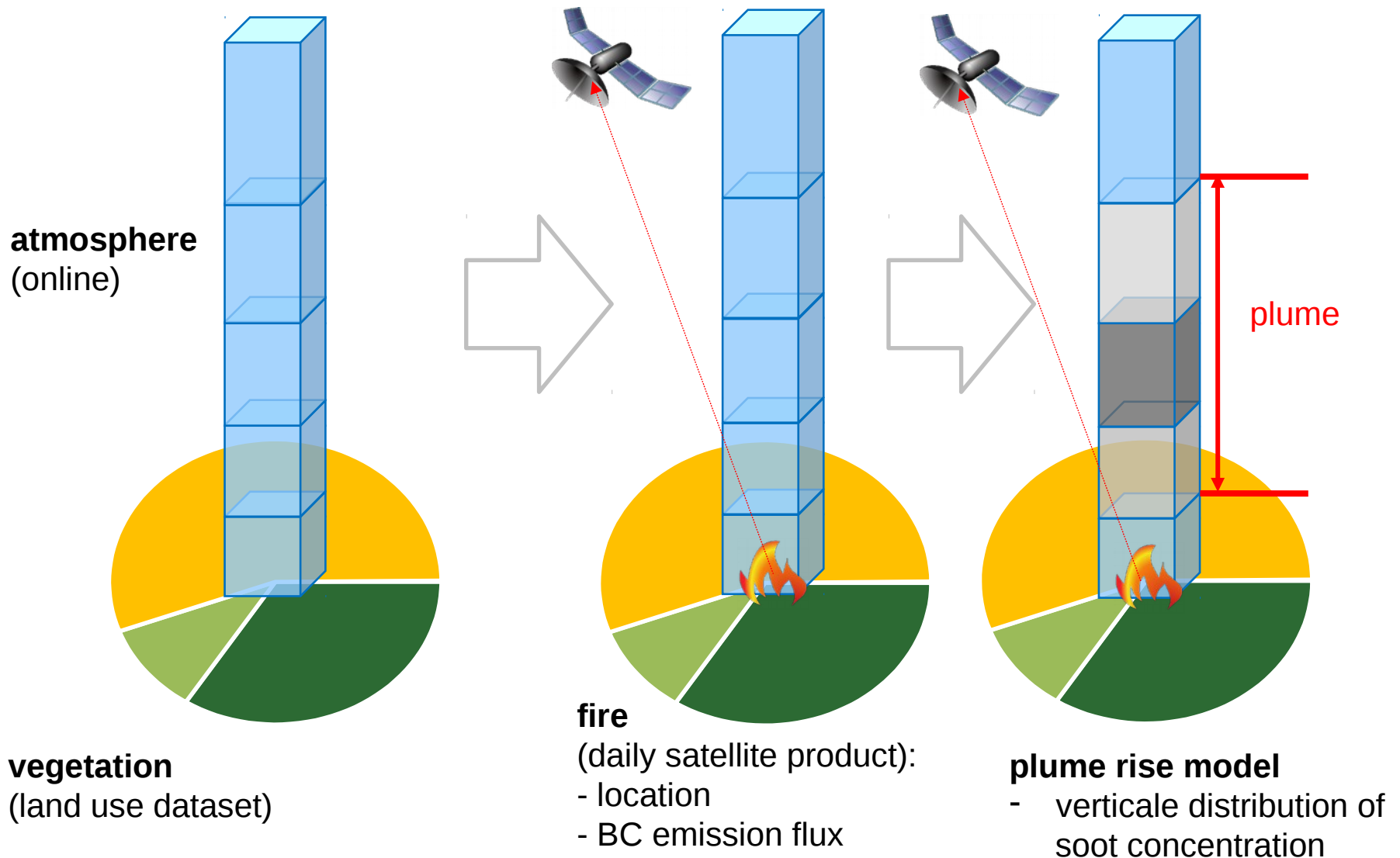


Portugal 2017

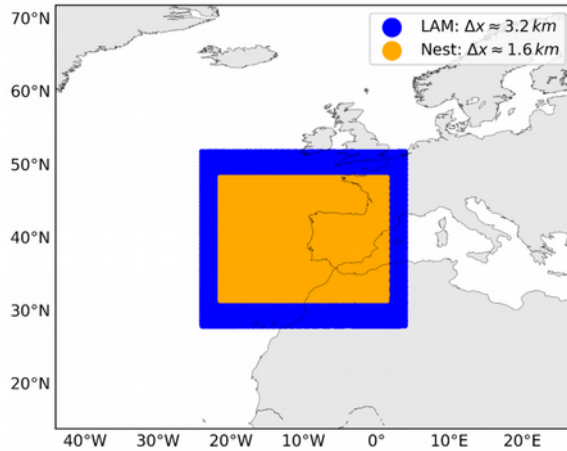


<https://worldview.earthdata.nasa.gov>

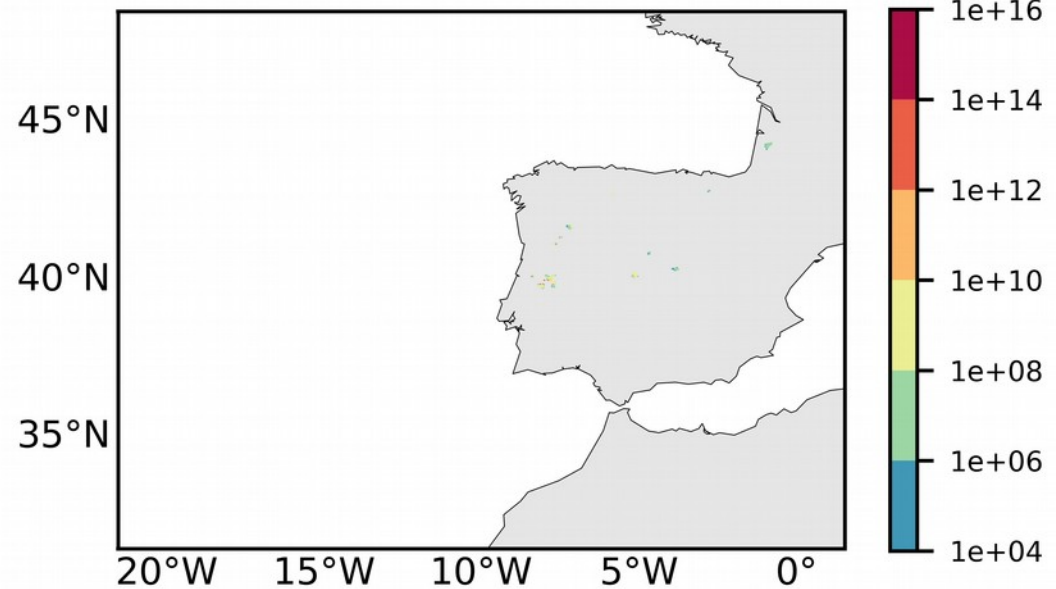
Plume rise model (Freitas et al. 2006, Walter et al. 2014)



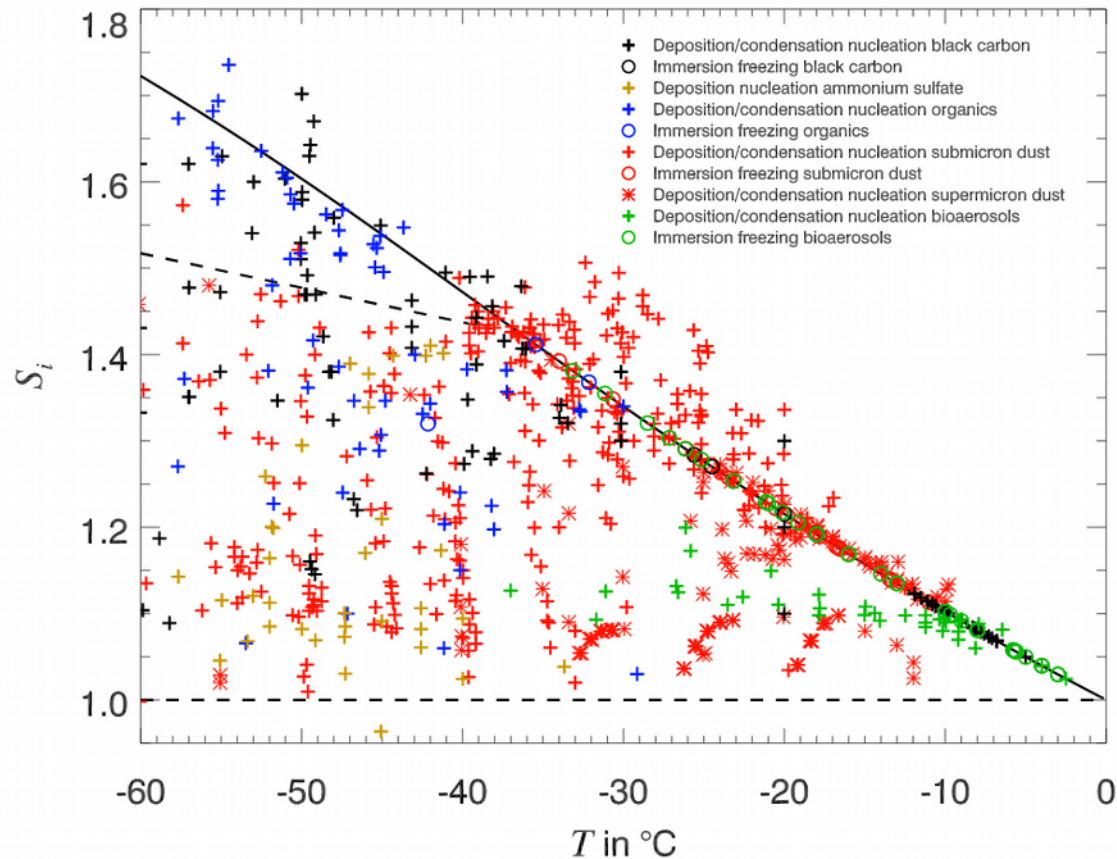
Portugal 2017



Vertical integrated soot ($\# m^{-2}$) 20170617-01UTC



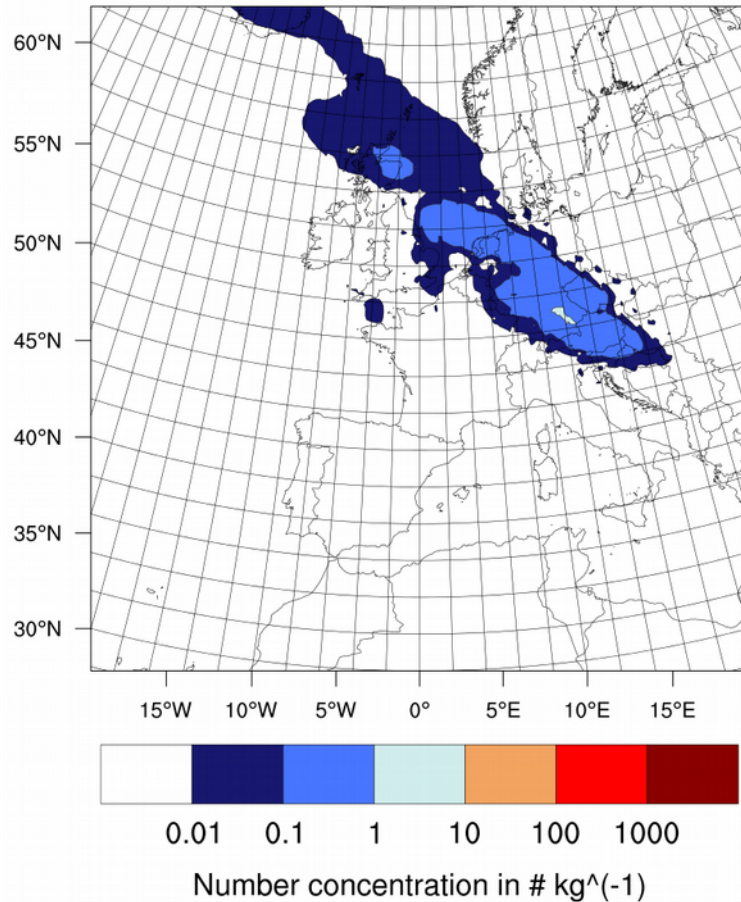
Overview of ice nucleation onset temperatures and saturation ratios



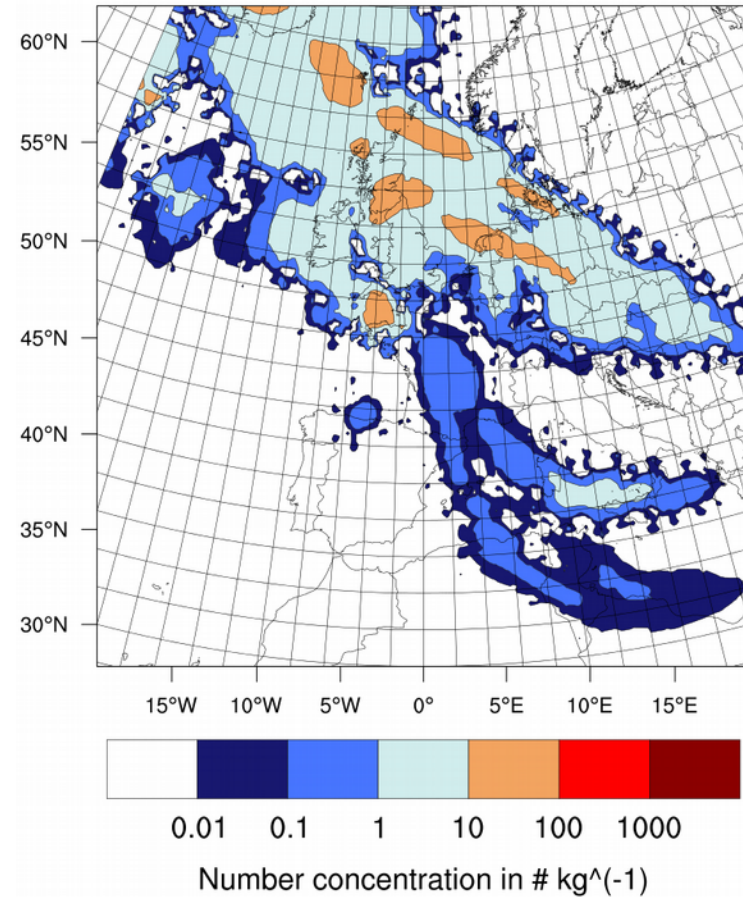
Hoose and Möhler, Atmos. Chem. Phys. Atmos. Chem. Phys., 12, 9817-9854,
<https://doi.org/10.5194/acp-12-9817-2012>, 2012

Horizontal distribution of pollen and sub-pollen

Contour plot - Pollen - Height: 8000 m

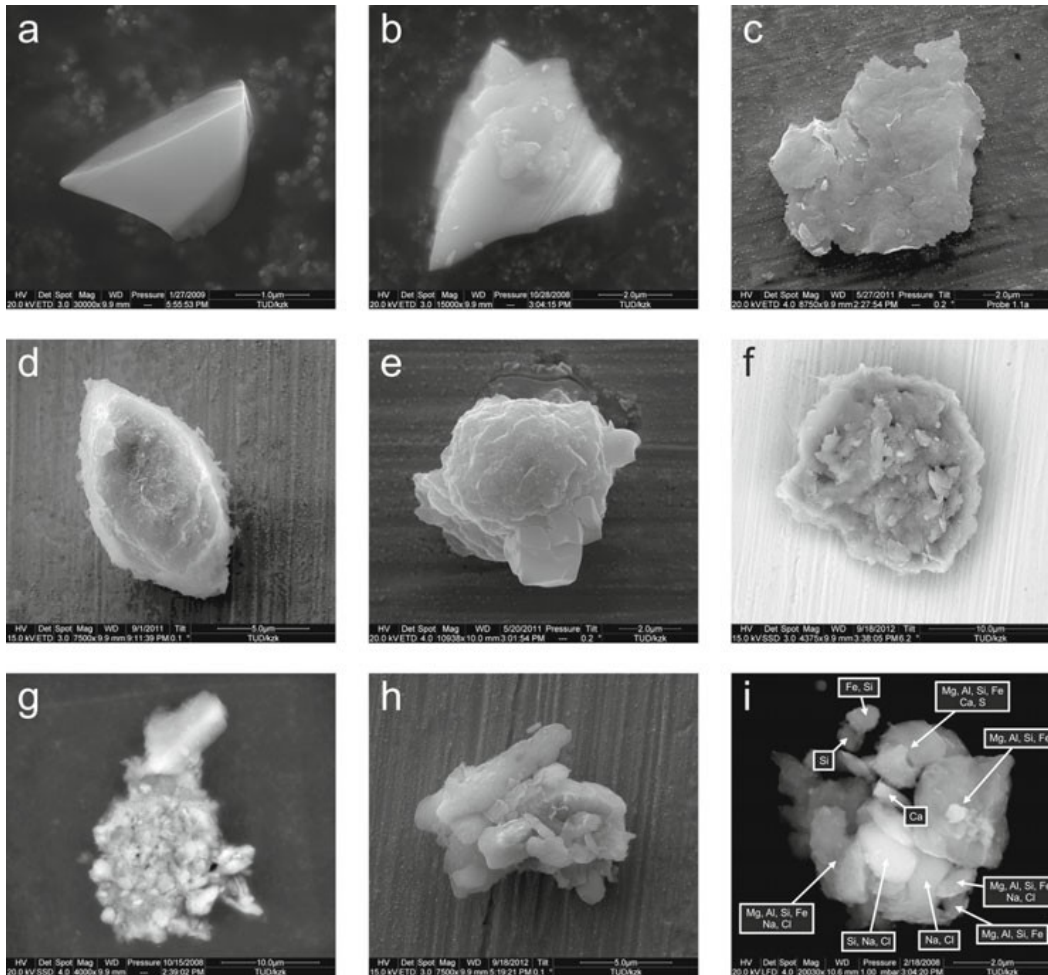


Contour plot - SPP - Height: 8000 m

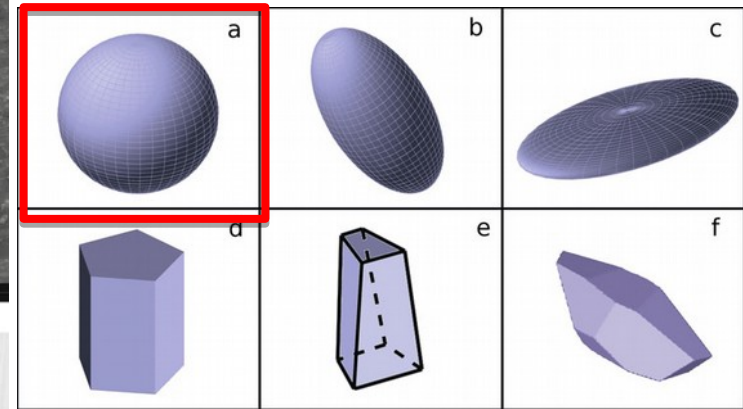


Dust particle shapes

Reality

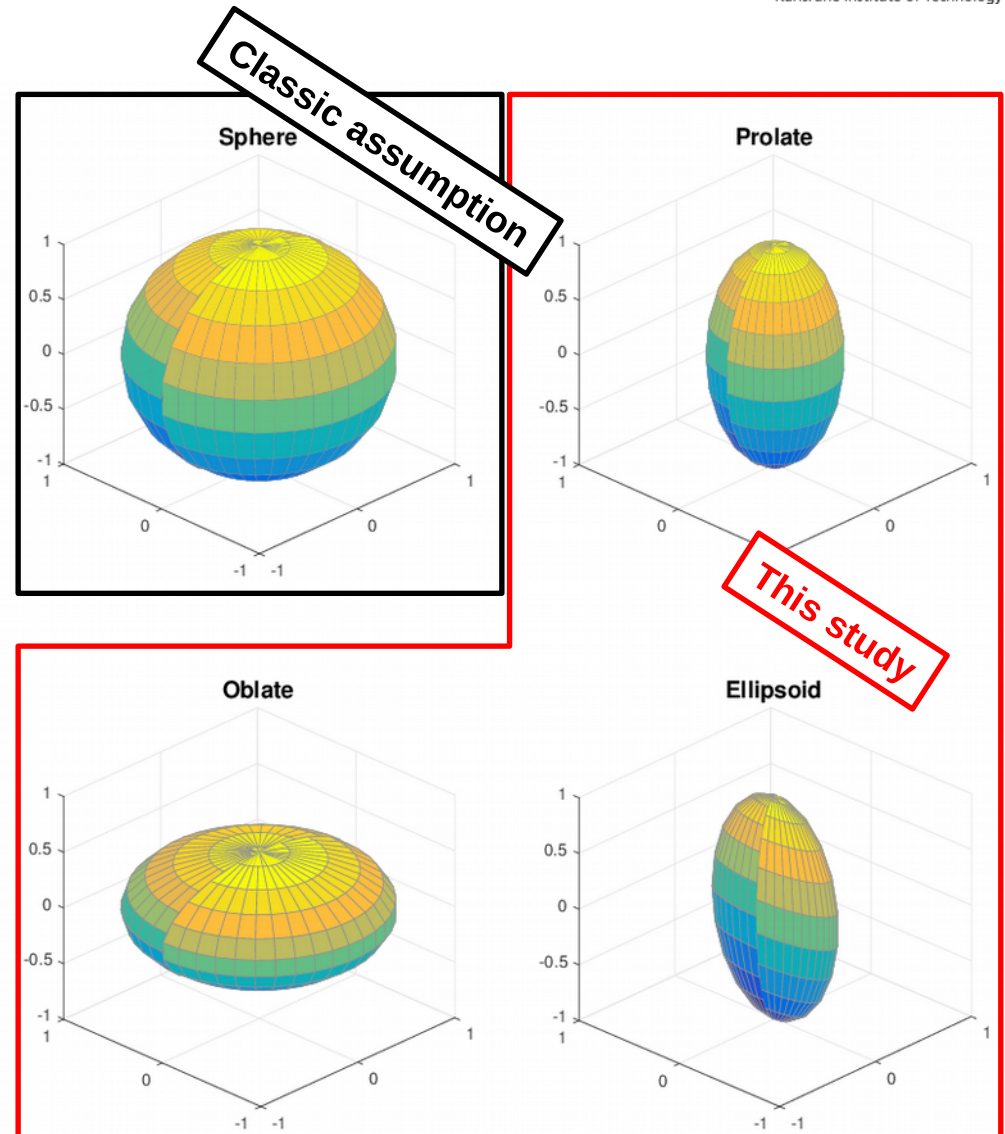


Models

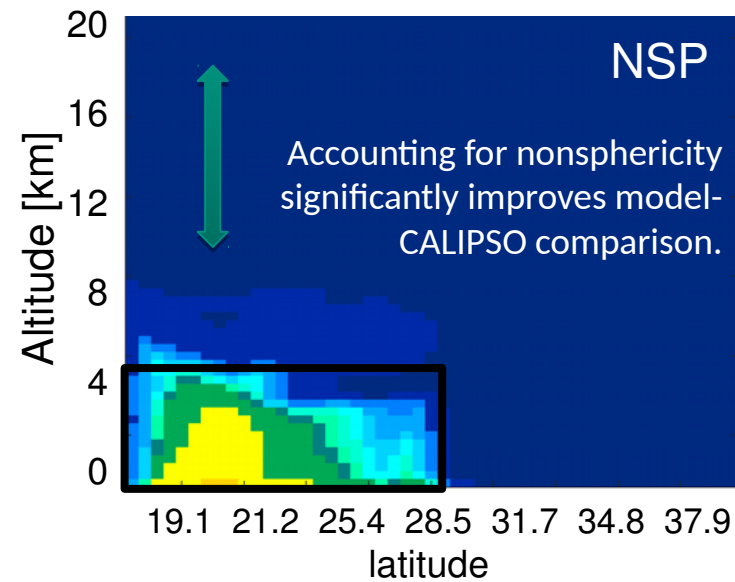
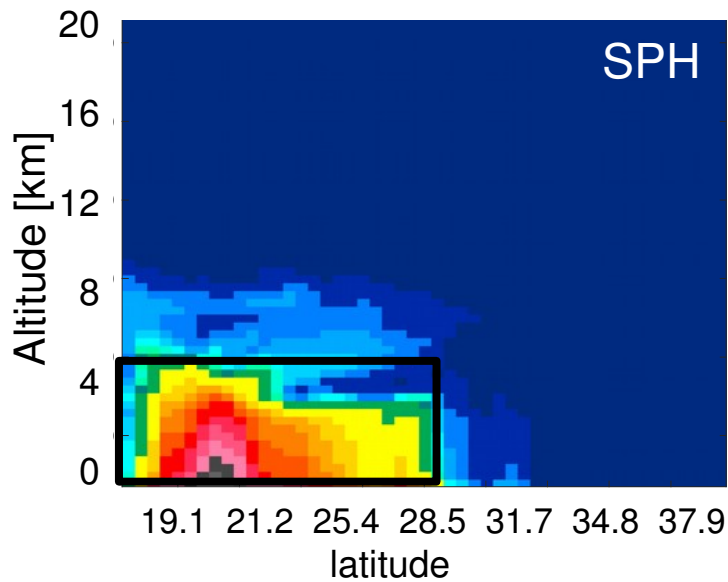
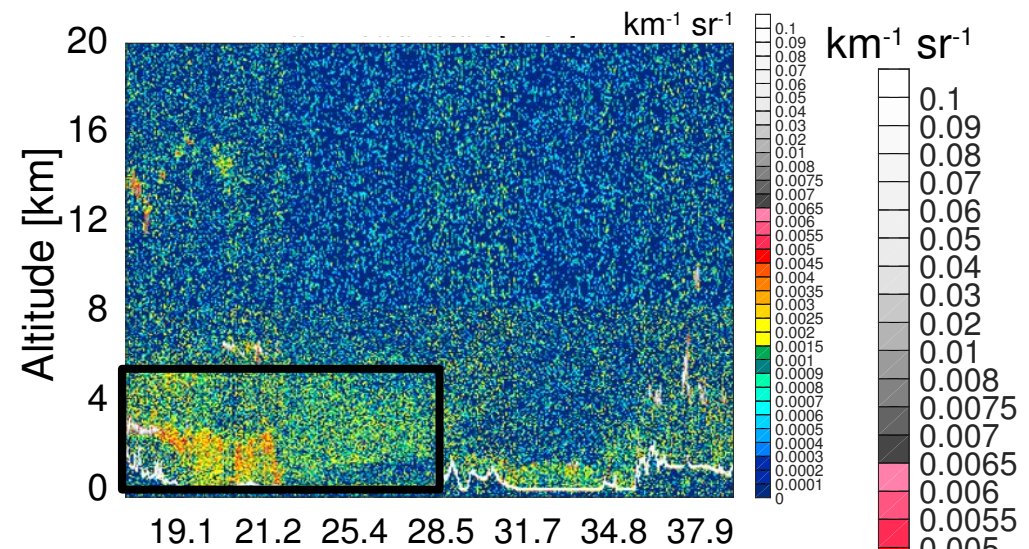
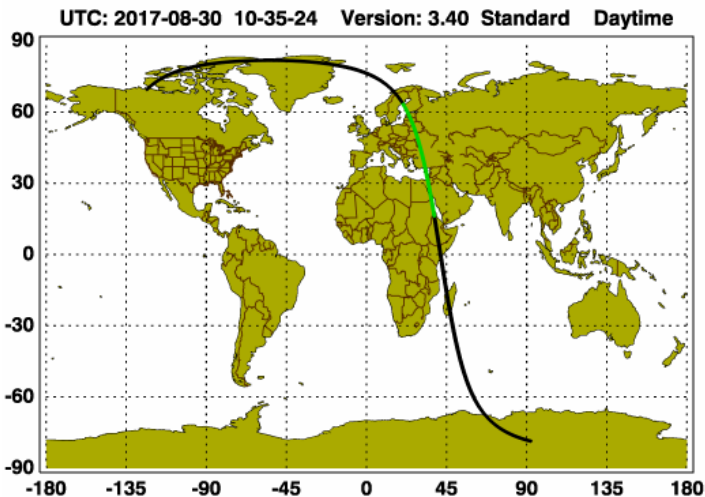


Dust forecast models usually assume spherical dust. But spheres fail to reproduce the magnitude and angular distribution of the scattering.

- **Tri-axial ellipsoids** better reproduce the laboratory measurements (Meng et al 2010).
- We use a mixture of 35 ellipsoid shapes with aspect ratio of 1.1 to 3.3.



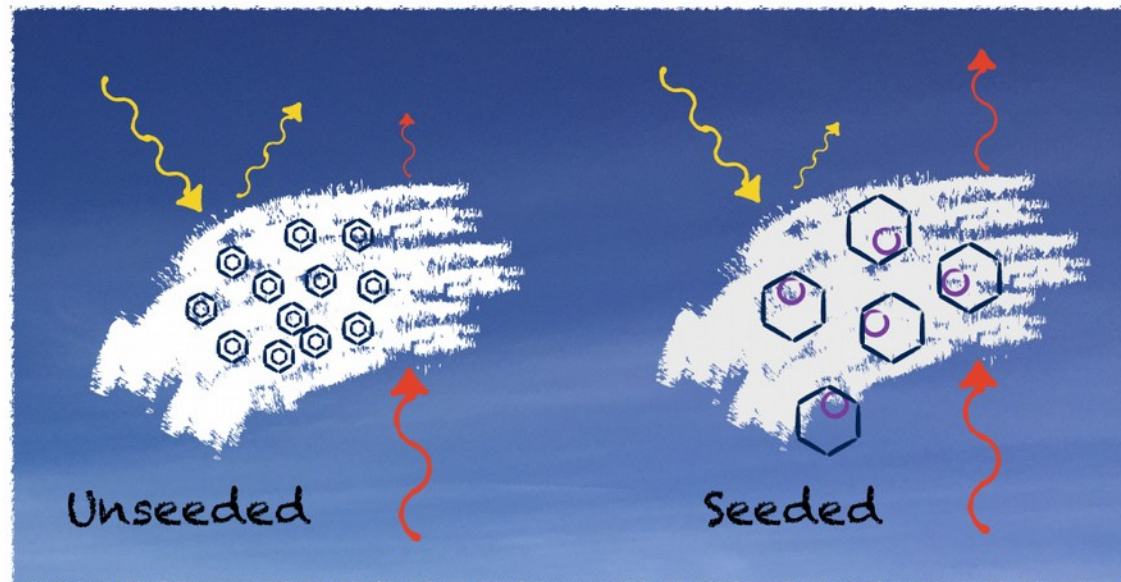
Verification: AB 1064 nm on 30.08.2017



- Improvement of ABS for NSP particles
- Minor changes for AOD
- Particle size distribution seems to be more important in case of AOD

Hoshyaripour, G., Bachmann, V., Förstner, J., Steiner, A., Vogel, H., Wagner, F., Vogel, B. Accounting for Particle Non-sphericity in a Dust Forecast System: Impacts on Model-Observation Comparison, submitted to JGR

Climate Engineering by Arctic Winter Cirrus Thinning

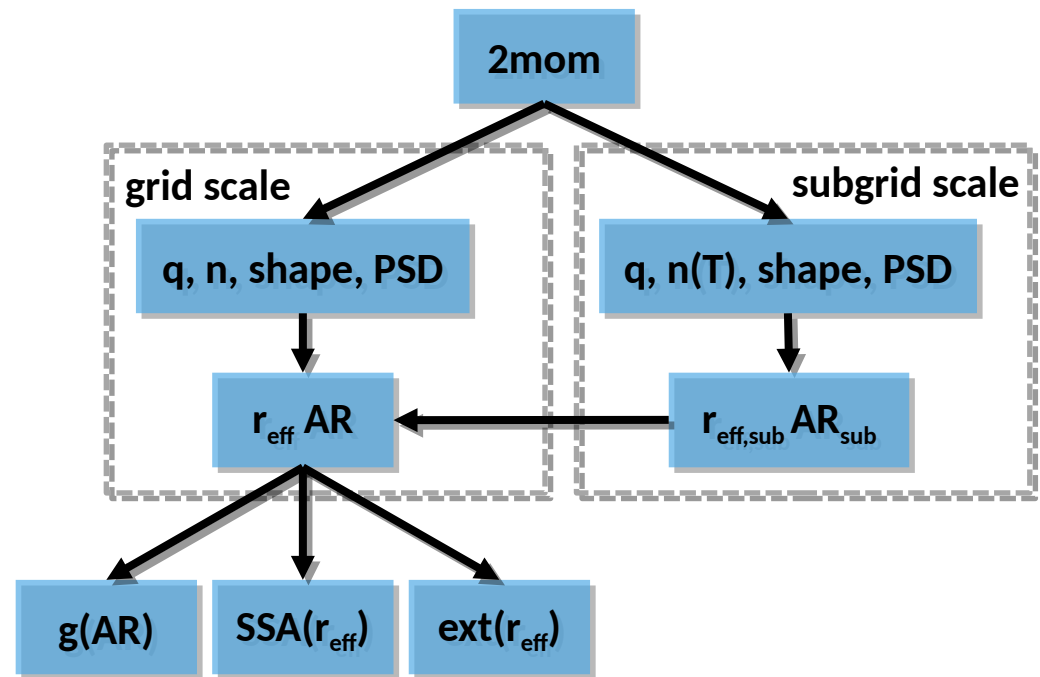
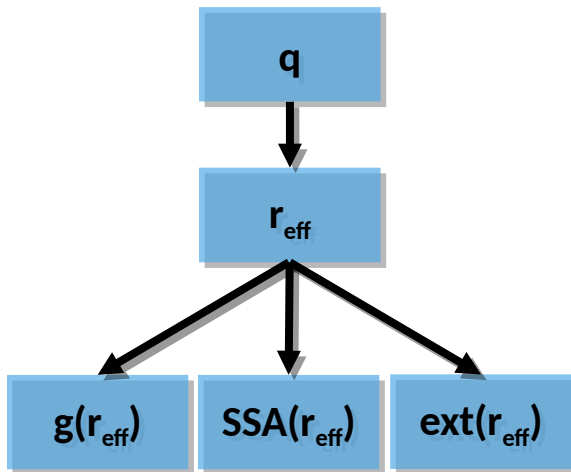


after Storelvmo et al., 2013

Optical Properties of Hydrometeors

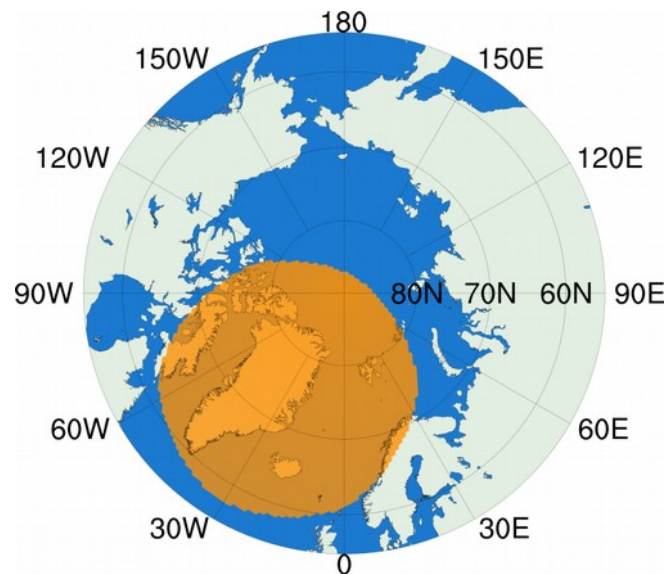
- old
- look-up tables of $r_{\text{eff}}(q)$
- cloud ice, cloud droplets

- new
- explicitly consider number conc.
- cloud ice, cloud droplets, rain, snow, graupel



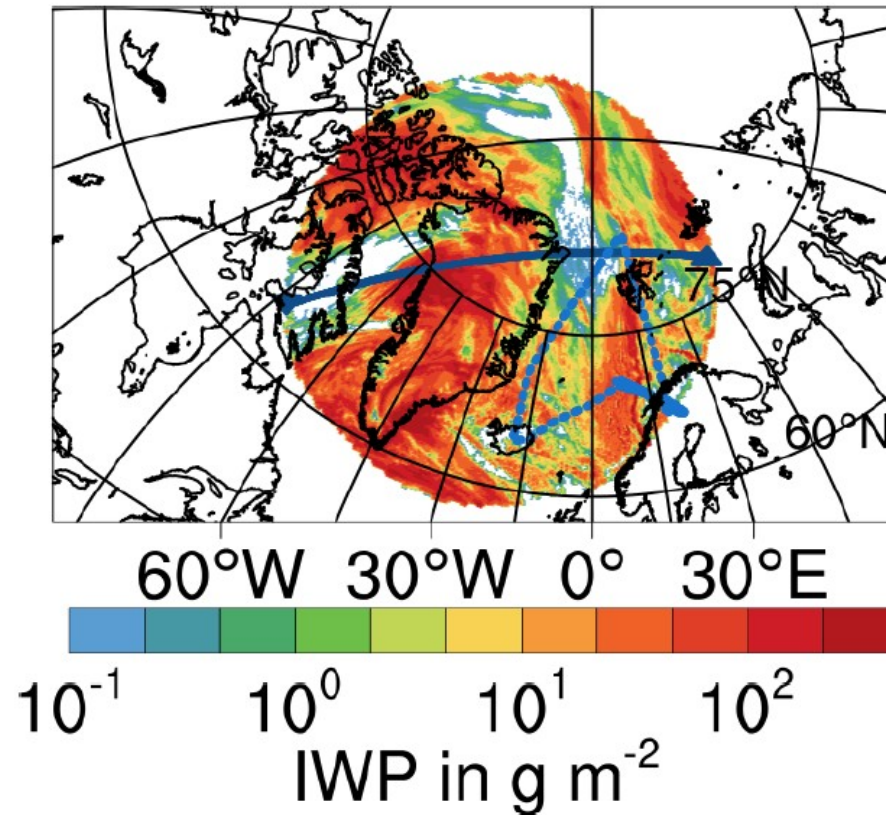
Model setup: ICON-ART LAM

- ❖ R2B09 (~5 km)
- ❖ two-moment microphysics: Seifert and Beheng (2006)
- ❖ cloud optical properties: Fu et al. (1998), Fu (2007), Hu and Stamnes (1993)
- ❖ nucleation: Barahona and Nenes (2009)
- ❖ heterogeneous nucleation: Phillips, et al. (2013)
- ❖ activation of CCN: Bangert et al. (2012)

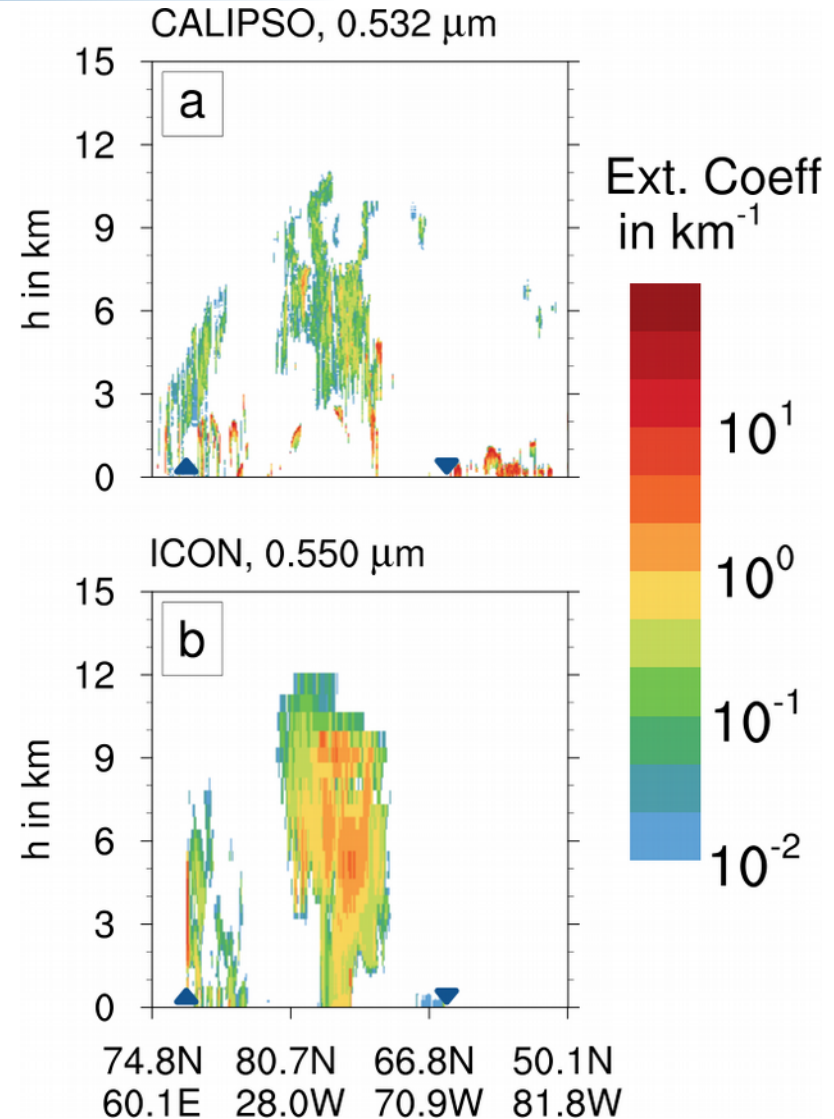
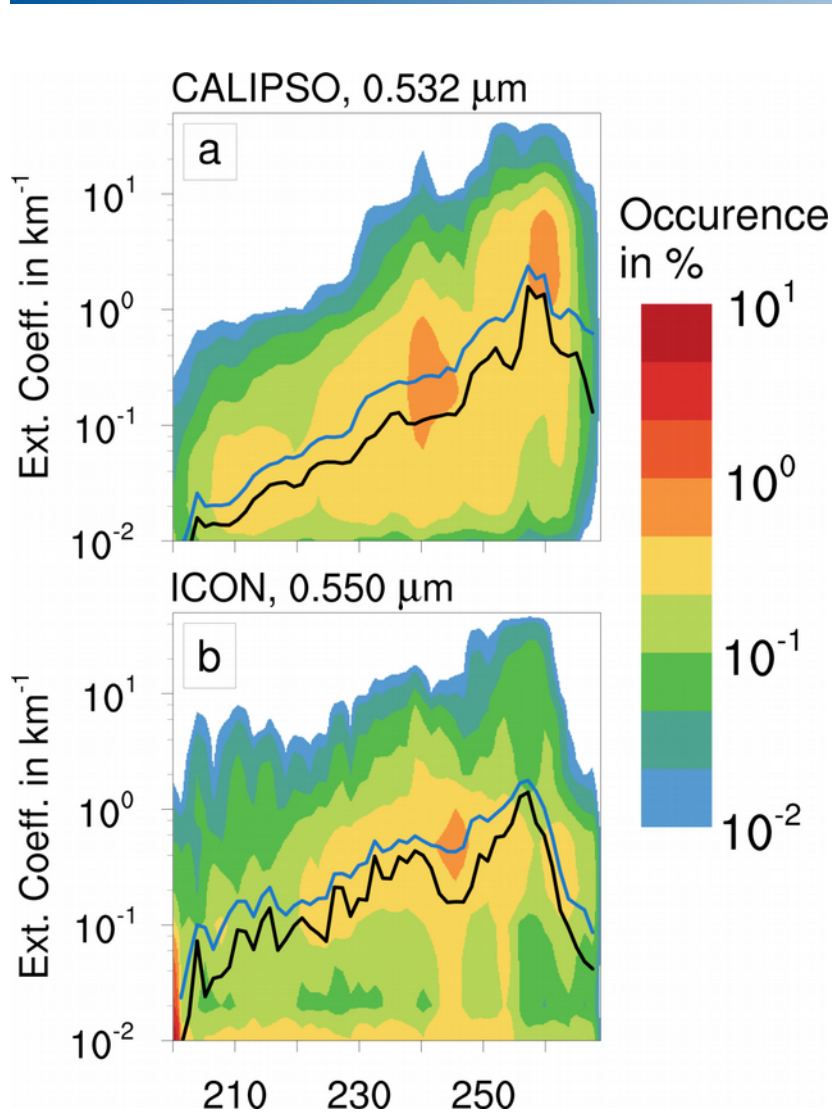


Gruber et al., 2018

Calipso and Halo flight tracks



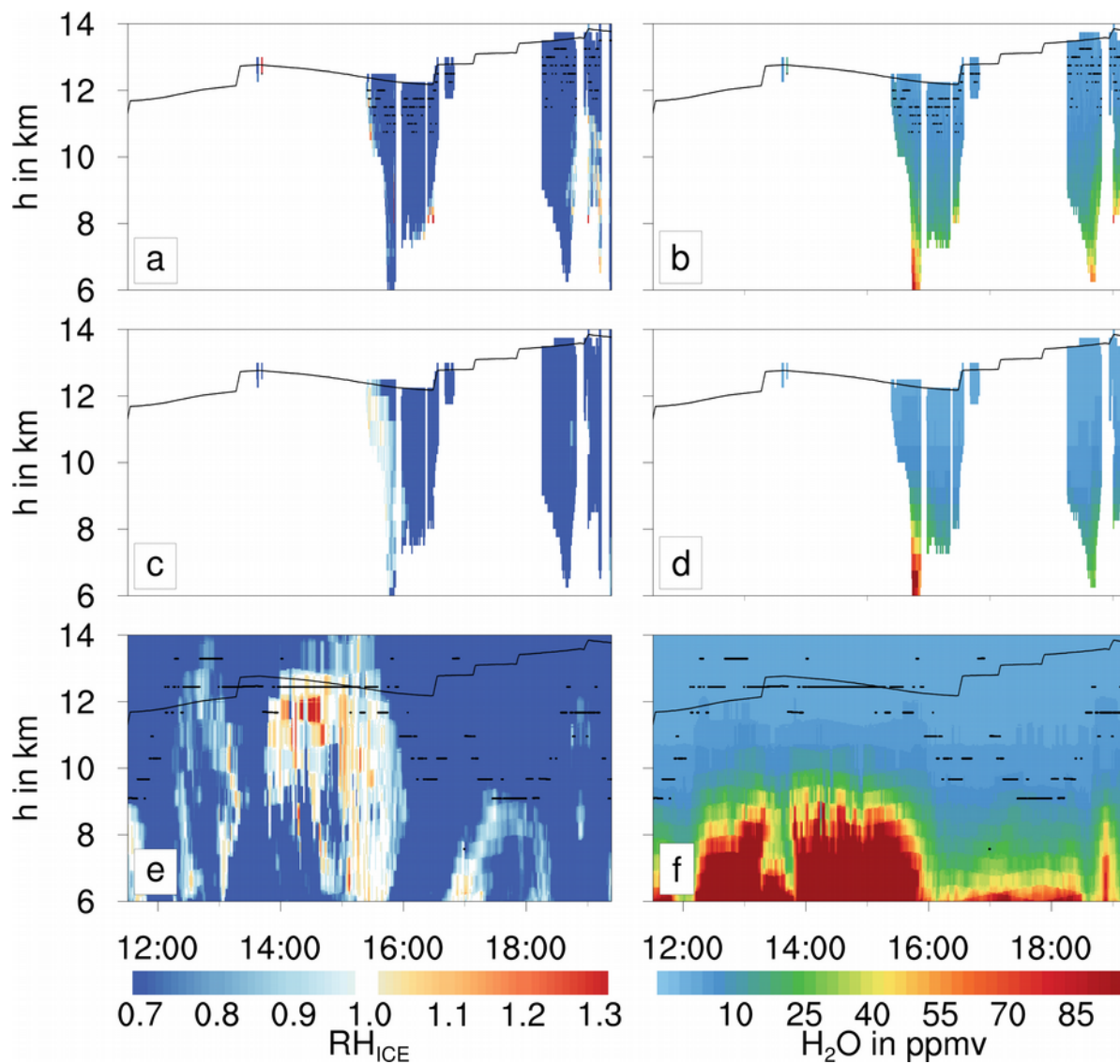
Validation: Calipso



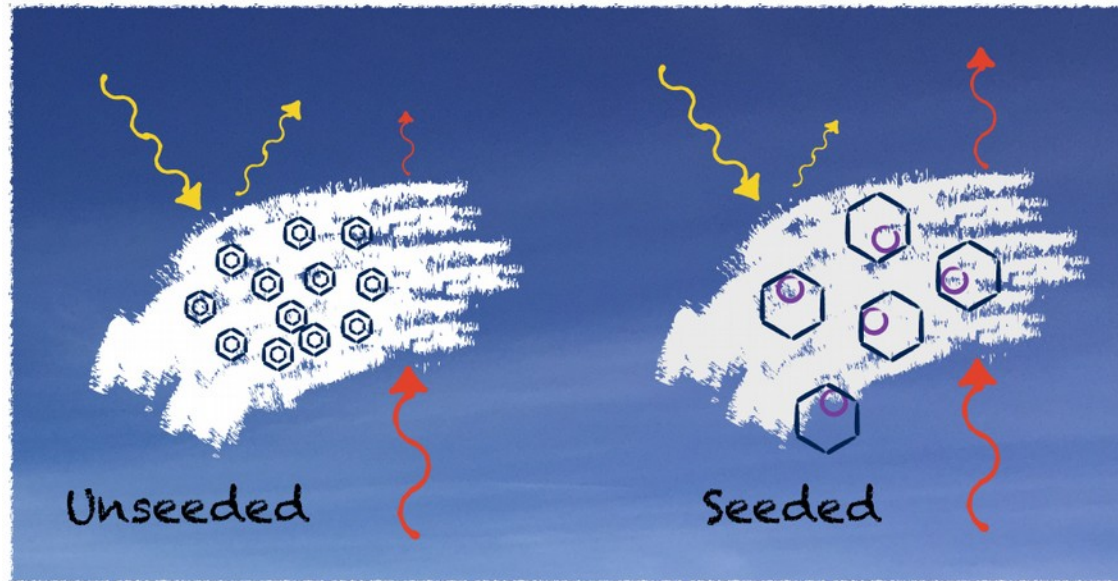
Validation: POLSTRACC, GLORIA

RH_{ice}

H_2O



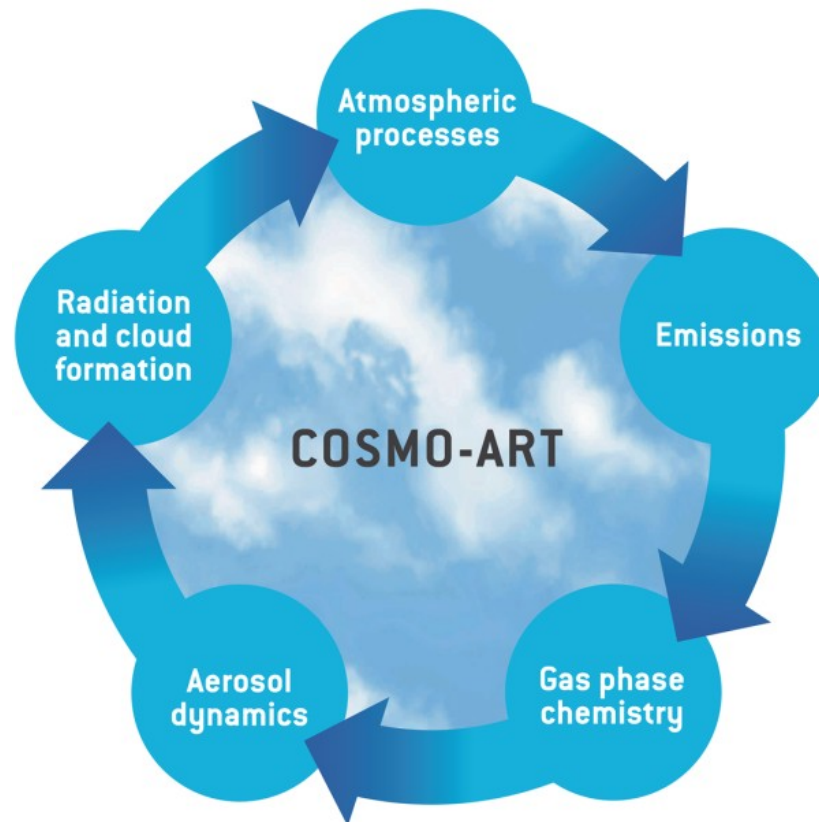
Climate Engineering by Arctic Winter Cirrus Thinning



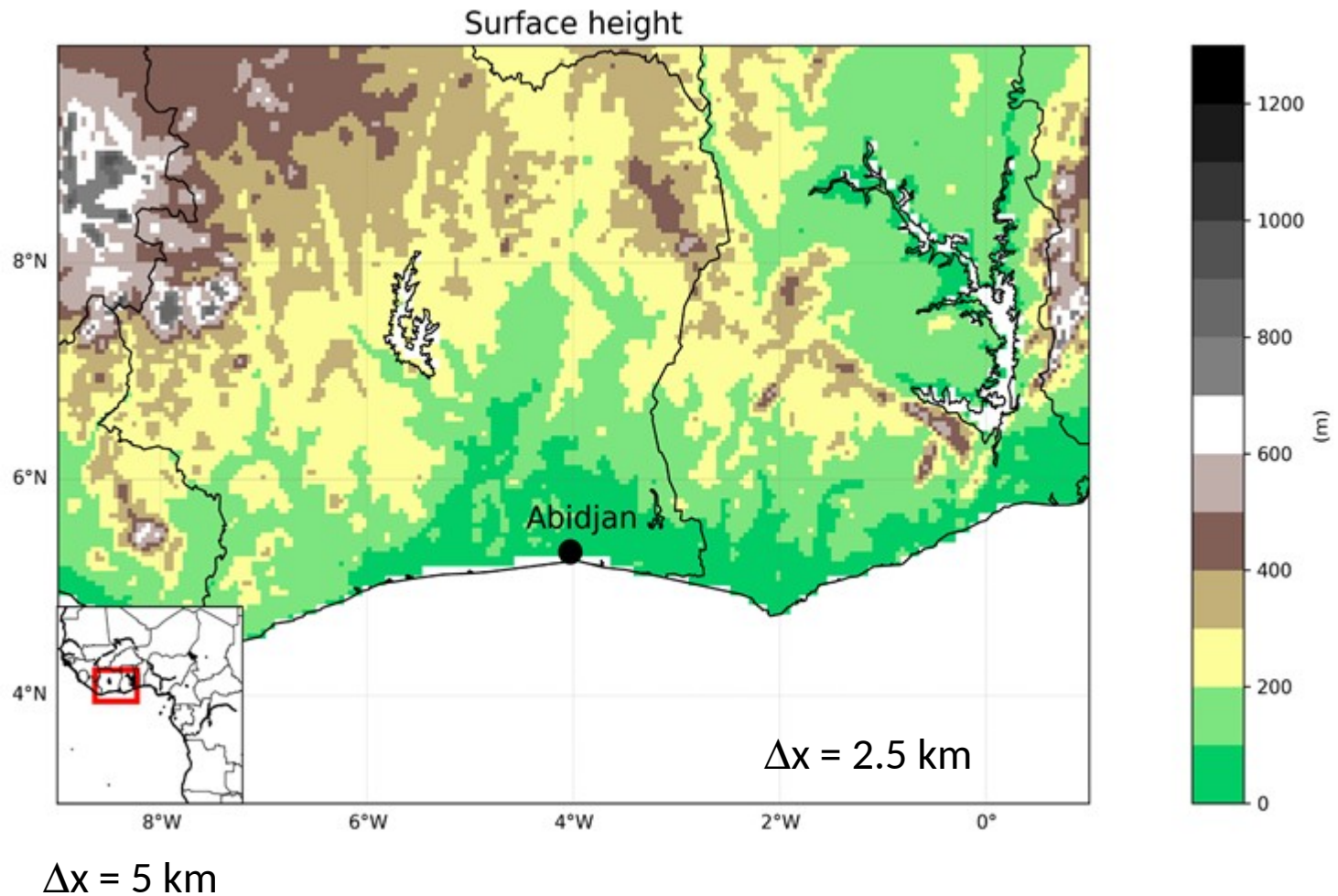
after Storelvmo et al., 2013

Gruber, S., U. Blahak, F. Haenel, Ch. Kottmeier, Th. Leisner, H. Muskatel, T. Storelvmo, and B. Vogel,
A process study on thinning of Arctic winter cirrus clouds with high-resolved ICON-ART simulations, in preparation

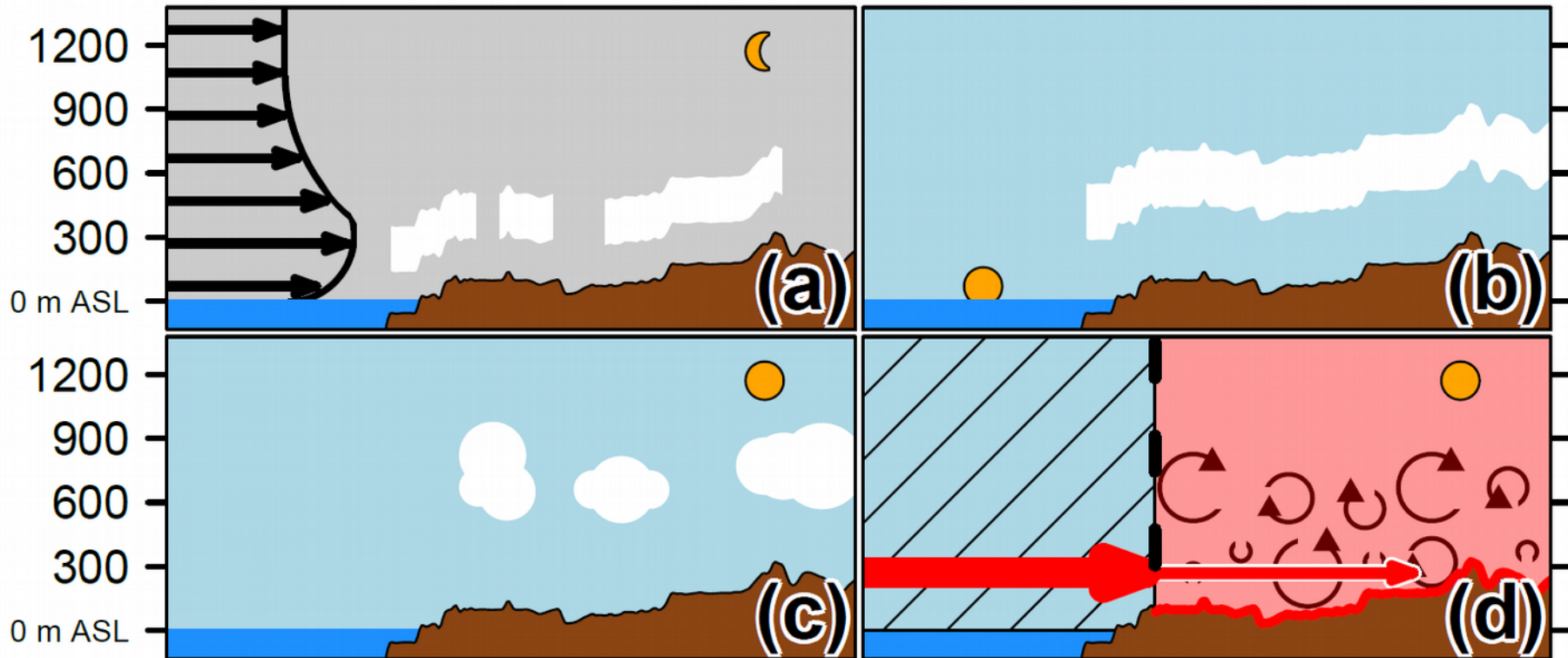
Applications of COSMO-ART



Impact of aerosols on clouds and atmospheric dynamics over southern West Africa



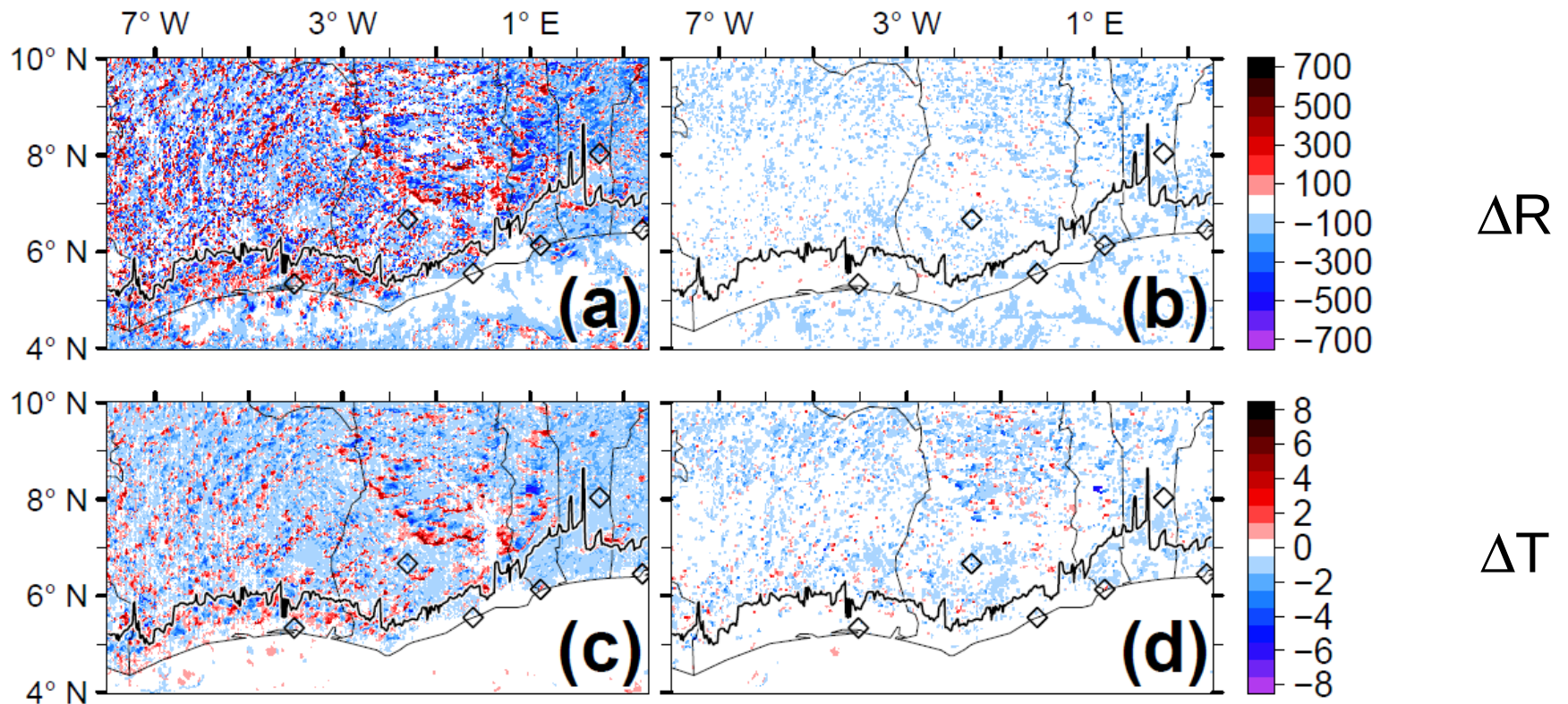
Deetz et al., 2018



Deetz et al., 2018 ACP

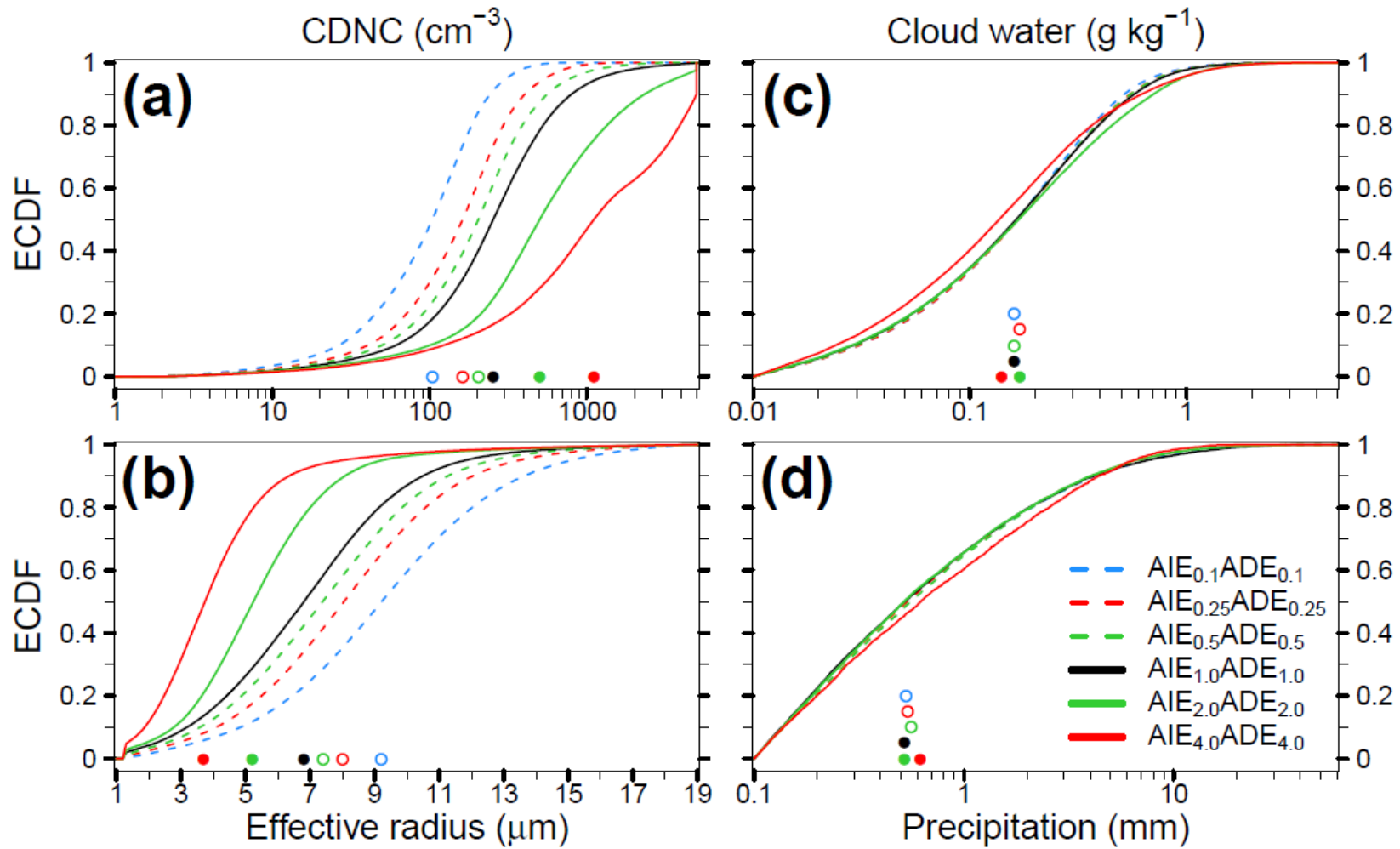
Abbreviation	Description of Simulation
$AIE_{0.1}ADE_{0.1}$	$F_{AIE} = 0.1$ and $F_{ADE} = 0.1$
$AIE_{0.25}ADE_{0.25}$	$F_{AIE} = 0.25$ and $F_{ADE} = 0.25$ (clean case)
$AIE_{0.5}ADE_{0.5}$	$F_{AIE} = 0.5$ and $F_{ADE} = 0.5$
$AIE_{1.0}ADE_{1.0}$	$F_{AIE} = 1.0$ and $F_{ADE} = 1.0$ (reference case)
$AIE_{2.0}ADE_{2.0}$	$F_{AIE} = 2.0$ and $F_{ADE} = 2.0$
$AIE_{4.0}ADE_{4.0}$	$F_{AIE} = 4.0$ and $F_{ADE} = 4.0$ (polluted case)

Impact on radiation

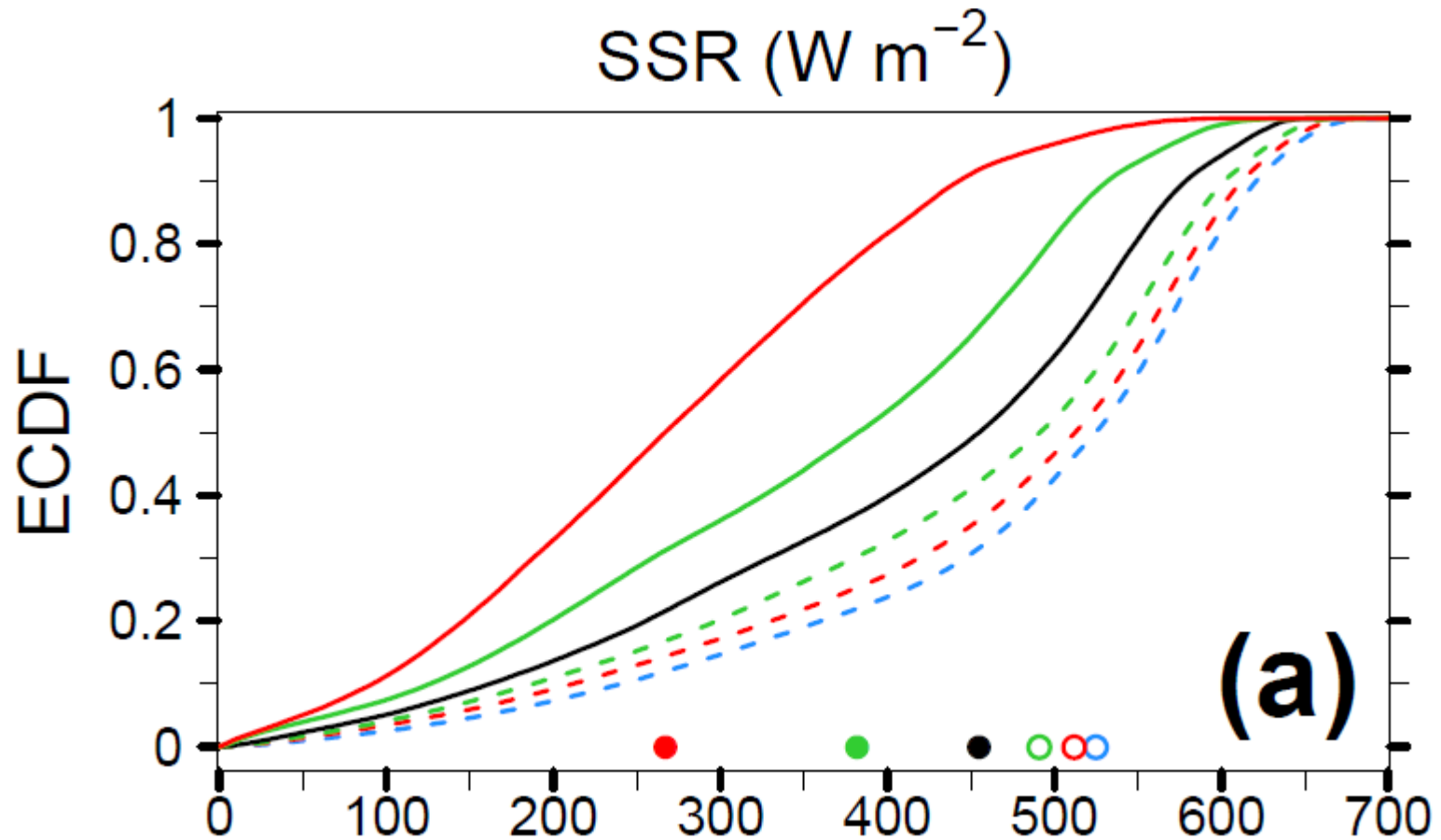


Deetz et al., 2018 ACP





Impact on physical properties and precipitation



Deetz et al., 2018 ACP



Deetz et al., 2018 ACP

-  **Aerosol strongly effects cloud effective radii.**
-  **LWC and precipitation show no significant change.**
-  **Strong impact of modified clouds on radiation.**
-  **Strong contribution from biomass burning in central Africa.**

K. Deetz, H. Vogel, P. Knippertz, B. Adler, J. Taylor, H. Coe, K. Bower, S. Haslett, M. Flynn, James Dorsey, Ian Crawford, Christoph Kottmeier, B. Vogel

Numerical simulations of aerosol radiative effects and their impact on clouds and atmospheric dynamics over southern West Africa, *Atmos. Chem. Phys.*, 18, 9767-9788, <https://doi.org/10.5194/acp-18-9767-2018>, 2018

K. Deetz, H. Vogel, S. Haslett, P. Knippertz, H. Coe, B. Vogel

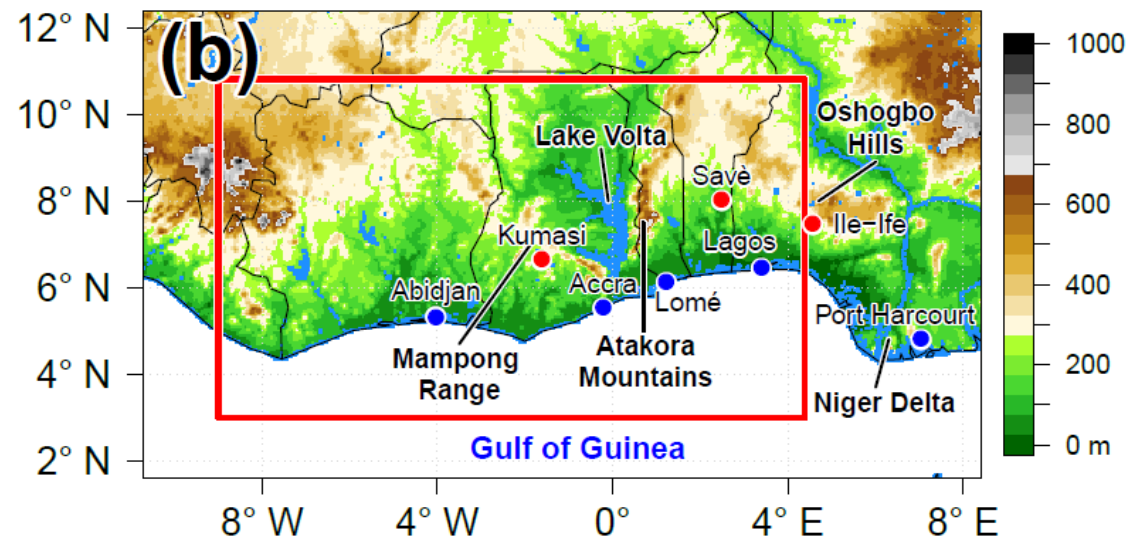
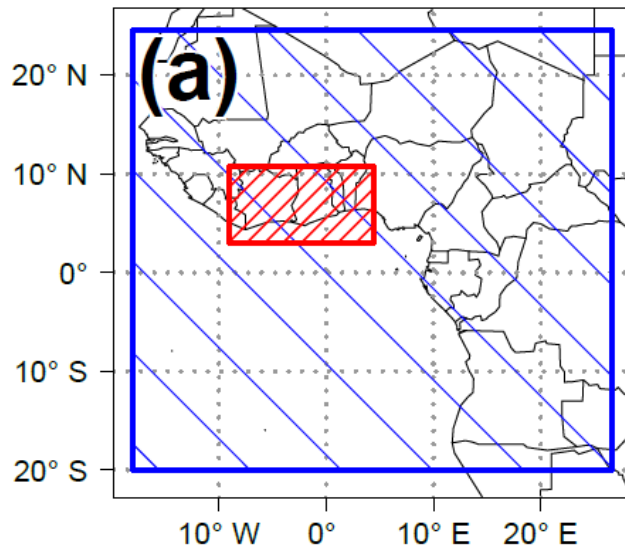
Aerosol liquid water content in the moist southern West African monsoon layer and its radiative impact *Atmos. Chem. Phys. Discuss.*, <https://doi.org/10.5194/acp-2018-420>, 2018



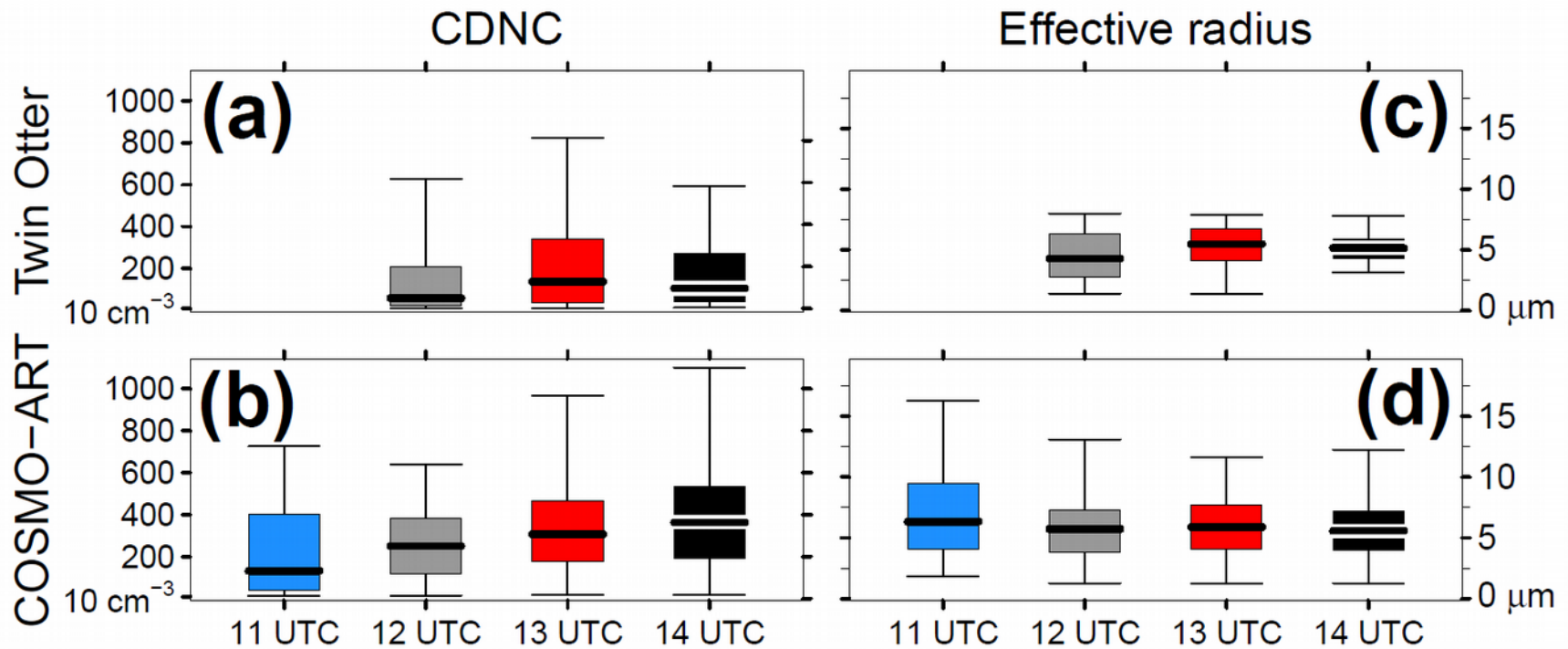
Research themes

- Impact of volcanic ash on atmospheric processes
 - Dust-cloud-radiation feedback
 - Scale dependency of aerosol cloud interaction
 - Climate engineering
 - Biomass burning aerosol
 - Impact of sub pollen particles
-
- Emission driven annual cycles
 - Chemistry-climate interactions, including PSCs
 - Water isotopologues (weather/climate)
 - Composition assimilation

Additional material Africa simulations

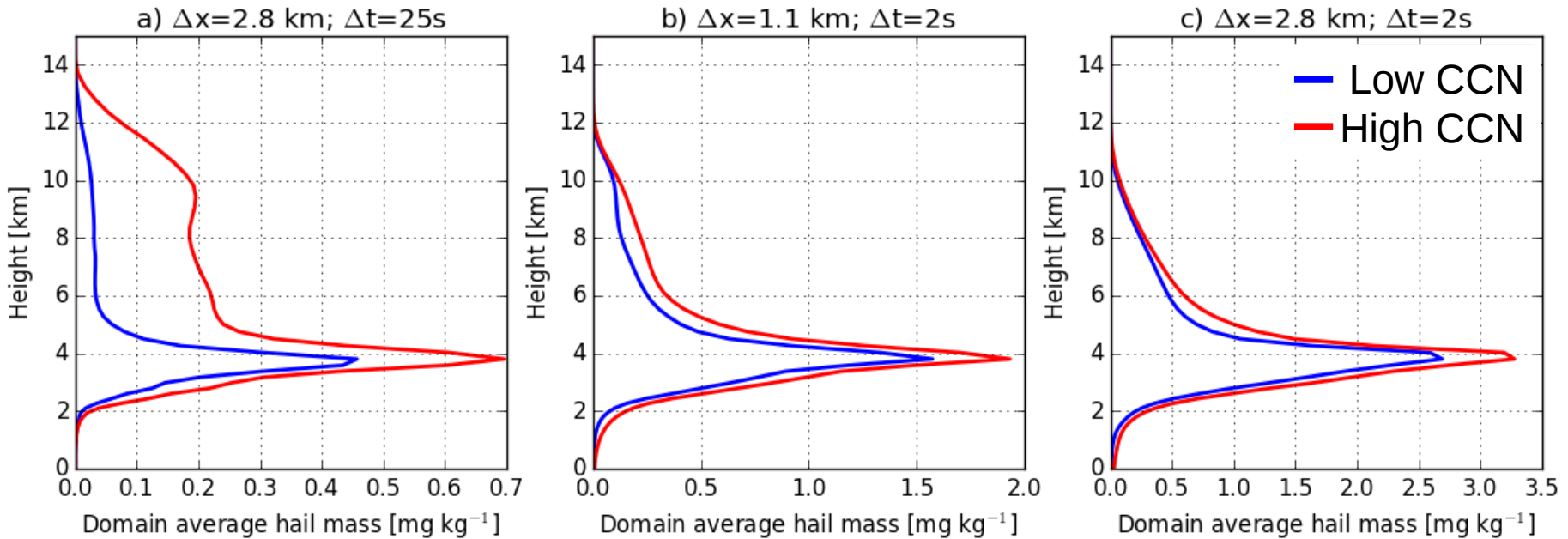


Comparison to observations



Additional material time spitting

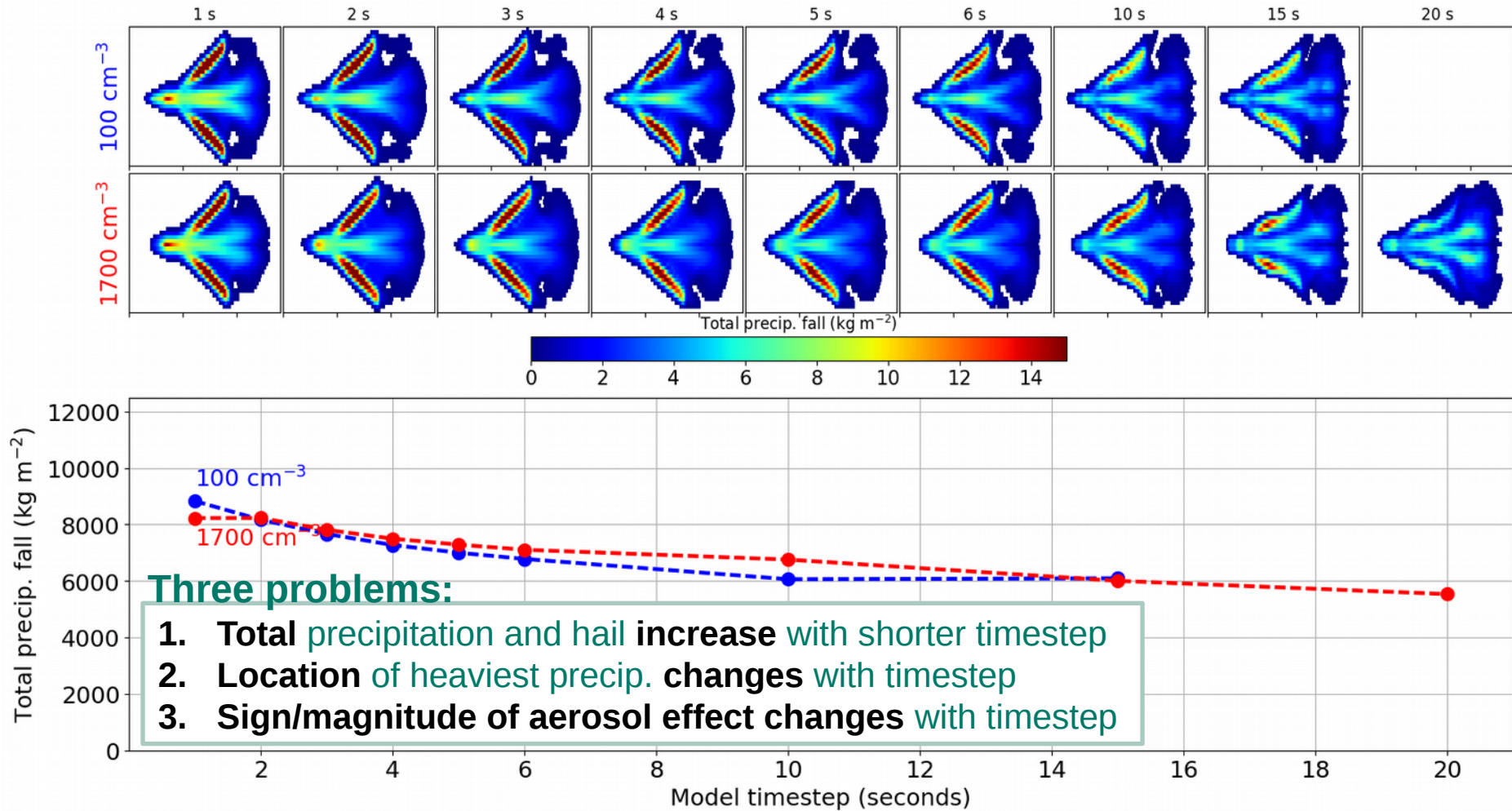
Microphysics sensitivity to timestep



Model setup

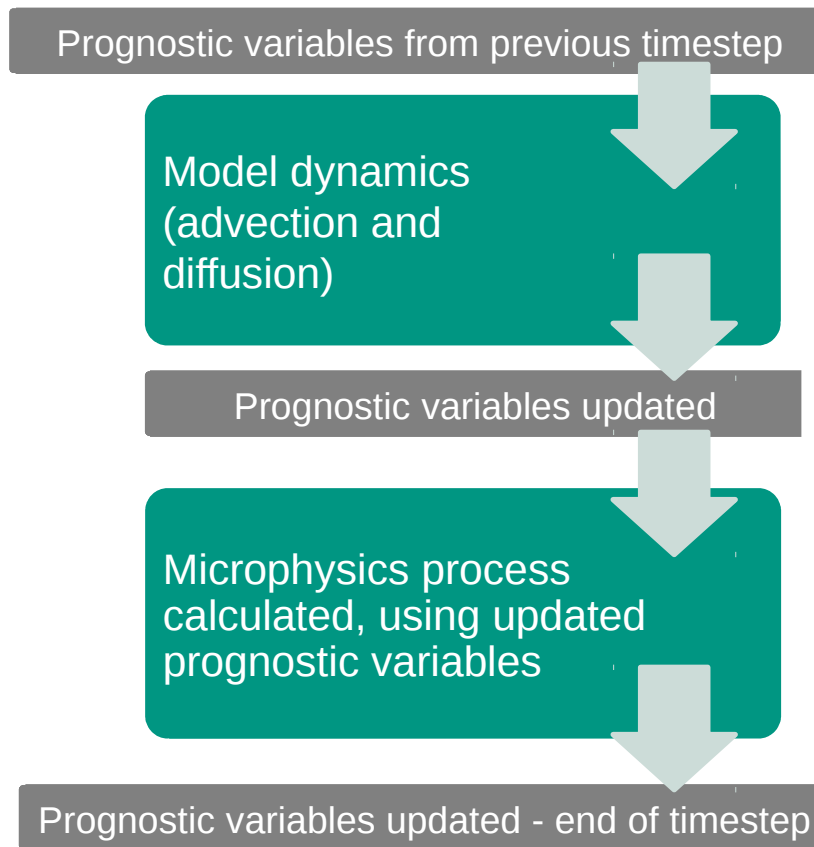
- Idealised 2-hour simulation using COSMO v5.3
- 1-km resolution; 64 vertical levels; timestep 1-20 s
 - Weisman-Klemp thermodynamic profile; 2K warm bubble; linear shear
- Seifert & Beheng 2-moment microphysics – Segal & Khain CCN activation
 - Two different aerosol settings:
 - clean = 100 CCN cm⁻³; continental = 1700 CCN cm⁻³

Total precipitation: aerosol and timestep effects



Why? Numerics!

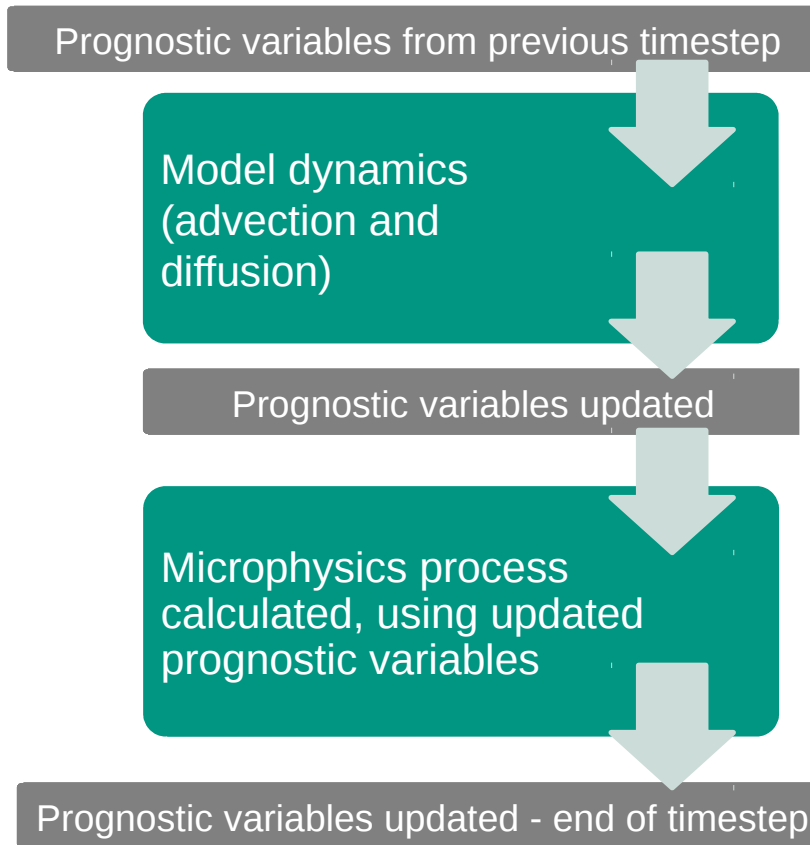
- Model dynamics calculated before microphysics



- Storm updraft -> adiabatic cooling
 - cooling -> supersaturation
 - Cooling = rate $\times \Delta t$
 - Supersaturation depends on timestep
-
- Microphysical processes now calculated using timestep-dependent supersaturation
 - Many processes affected
 - Timestep-dependent results

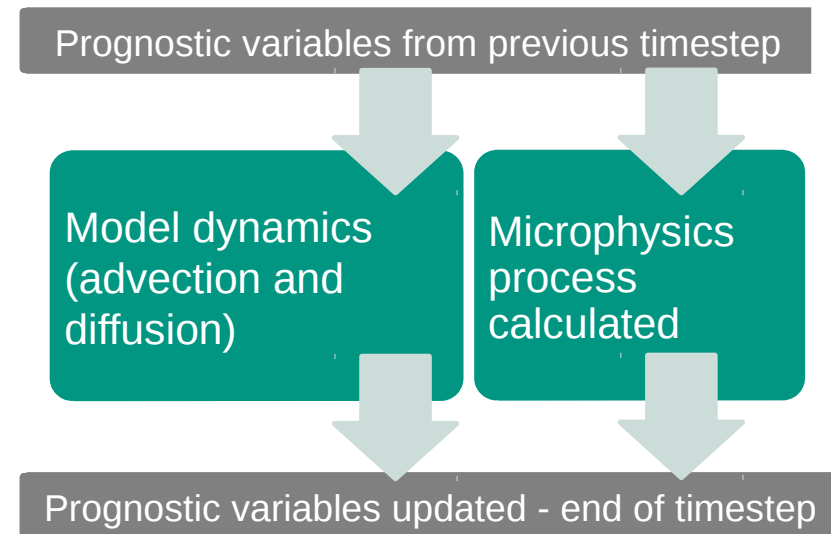
Operator Splitting: Consecutive vs Simultaneous

Process splitting in COSMO:



“Operator Splitting” or “Additive Splitting”

A different option:



“Additive Splitting”

Timestep dependence in a simple model

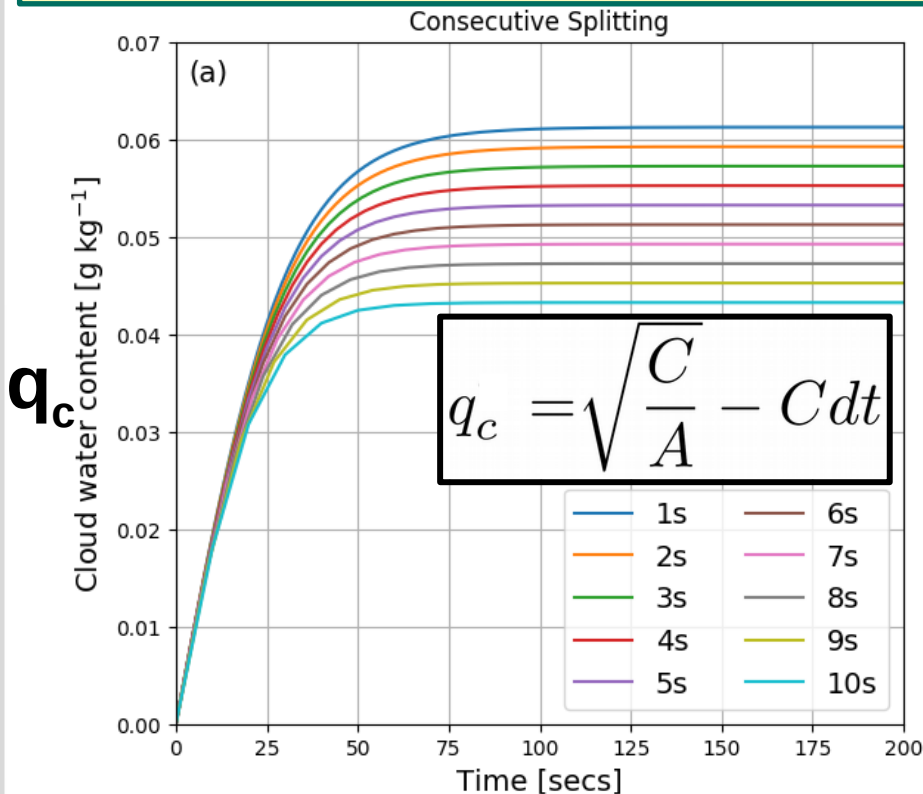
$$\frac{dq_c}{dt} = \underbrace{C}_{\text{Condensation}} - \underbrace{Aq_c^2}_{\text{Autoconversion (microphysics)}}$$

$q_c = \sqrt{\frac{C}{A}}$

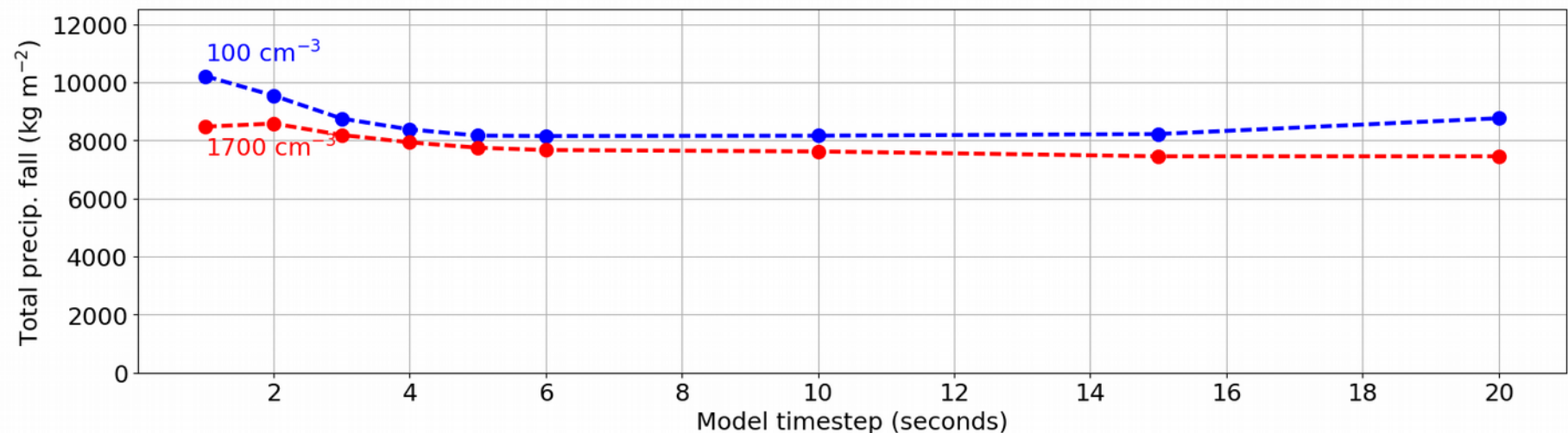
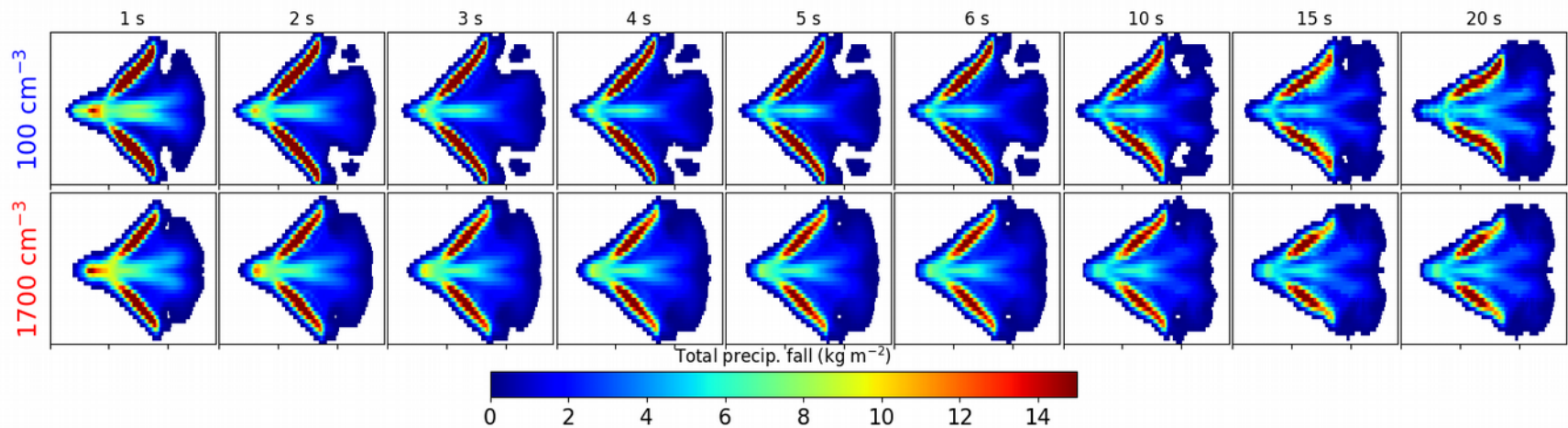
C = "Dynamics"

- Updraft
- □ cooling
- □ condensation

Aq_c² = "simplified microphysics"

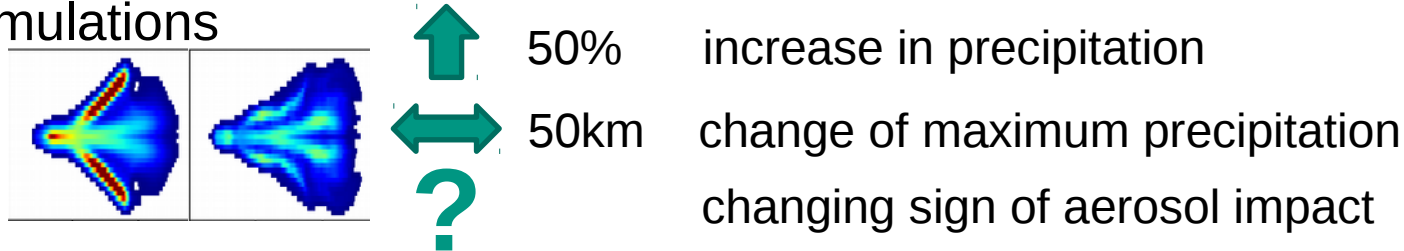


COSMO with Simultaneous Splitting

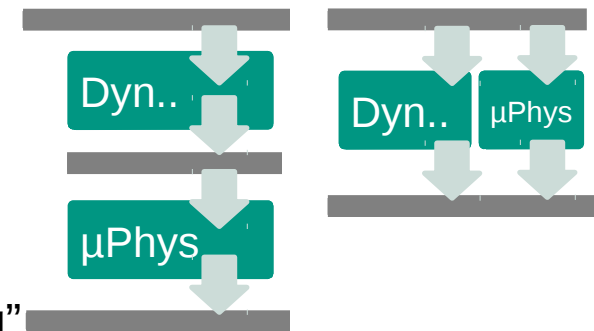


Summary

- Large and systematic effect of model timestep on convection-permitting simulations



- Caused by “Consecutive Splitting”
 - Dynamics calculated first, then microphysics
 - Supersaturation (or q_c) scales with timestep
 - Results much better with “Simultaneous Splitting”

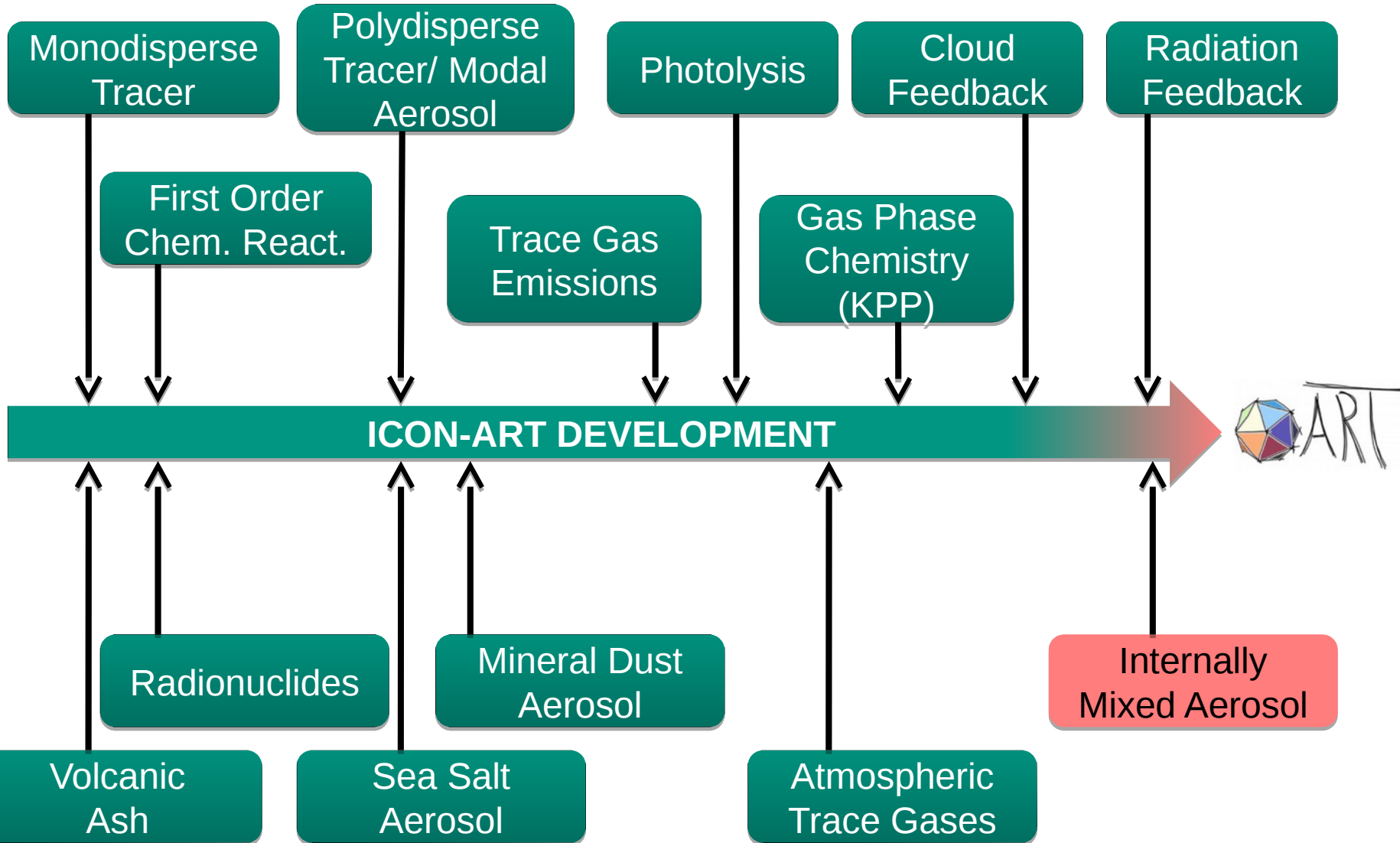


- Affecting convection-permitting simulations ... in most (all?) models
 - Also affects NWP and process-studies

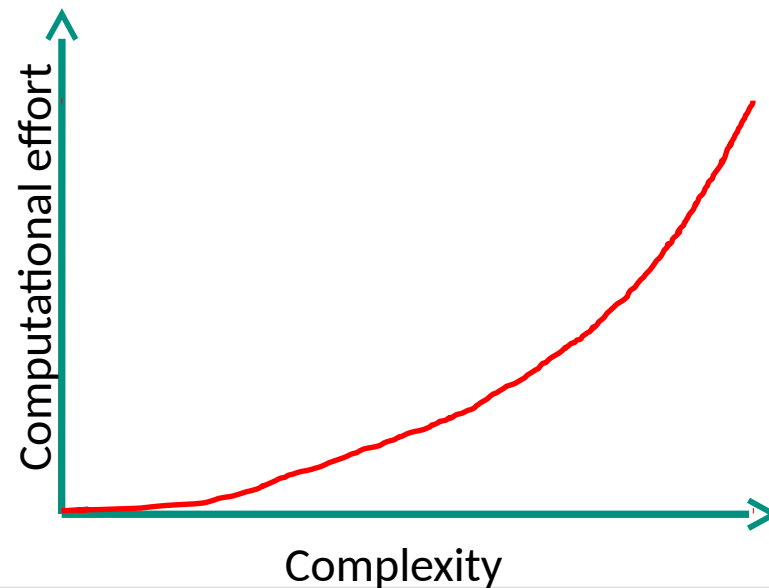
- Solution: Changing input for microphysics – easy to change in model

Additional material aerosol module

Milestones



- 🌐 **Aerosol, radiation and cloud physics**
- 🌐 **Convective uplift**
- 🌐 **Chemistry-climate feedbacks**



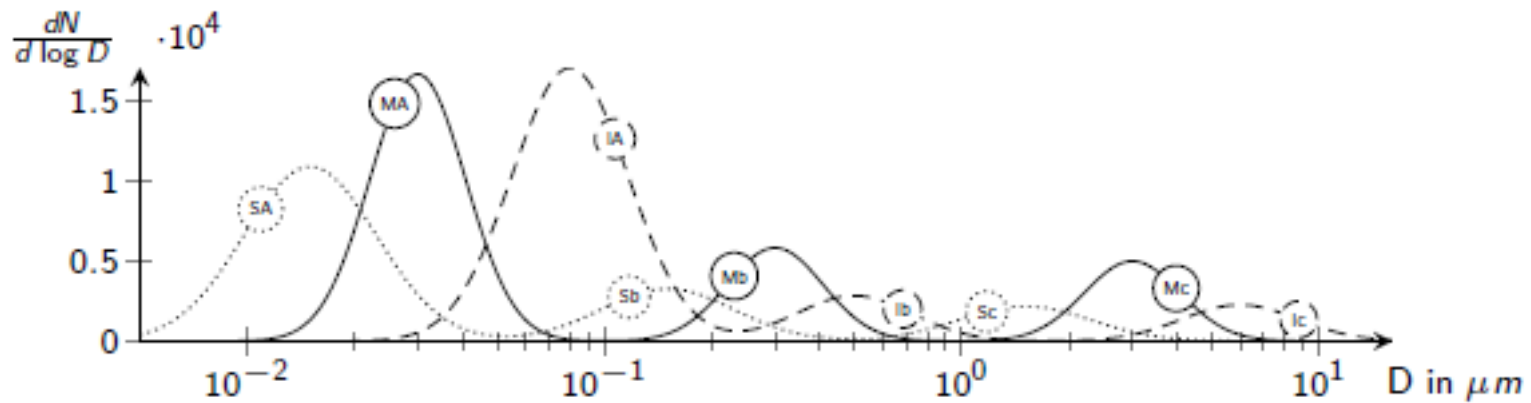
The basic equation

$$\begin{aligned}
 \frac{\partial n(v_P)}{\partial t} = & \underbrace{-\nabla \cdot \mathbf{v} n(v_P)}_{\text{Advection}} - \underbrace{\nabla \cdot \mathbf{c}_P(v_P) n(v_P)}_{\text{External forces}} + \underbrace{\nabla \cdot D_{PAR}(v_P) \nabla n(v_P)}_{\text{Diffusion}} \\
 & + \underbrace{\frac{1}{2} \int_0^{v_P} \beta(v_P - \tilde{v}_P, \tilde{v}_P) n(v_P - \tilde{v}_P) n(\tilde{v}_P) d\tilde{v}_P - \int_0^\infty \beta(v_P, \tilde{v}_P) n(v_P) n(\tilde{v}_P) d\tilde{v}_P}_{\text{Coagulation}} \\
 & + \underbrace{\left[\frac{\partial}{\partial t} n(v_P) \right]_g}_{\text{Particle growth}} + \underbrace{\dot{n}_S(v_P)}_{\text{Sources/sin}}
 \end{aligned}$$







Friedlander (1977)





SO₄ NH₄ NO₃ Na Cl POM SOA1 SOA2 SOA3 SOA4 H₂O
BC DU VA

Pol



Aitken mode accumulation mode coarse mode

-  **Atmospheric transport**
(advection, convection, turbulent diffusion)
-  **Sedimentation**
-  **Washout**
-  **Emission**
(sea salt, mineral dust, volcanic ash, pollen, radioactive material)
-  **Optical properties**
-  **Activation**

-  **Coagulation**
-  **Condensation (explicit of H_2SO_4)**
-  **Nucleation**
-  **Gas-aerosol partitioning**

Coagulation

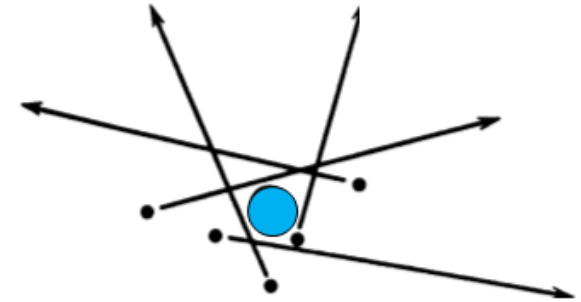
	SA	IA	MA	Sa	Ia	Ma	Sc	Ic	Mc
SA	SA	MA	MA	Sa	Ma	Ma	Sc	Mc	Mc
IA		IA	MA	Ma	Ia	Ma	Mc	Ic	Mc
MA			MA	Ma	Ma	Ma	Mc	Mc	Mc
Sa				Sa	Ma	Ma	Sc	Mc	Mc
Ia					Ia	Ma	Mc	Ic	Mc
Ma						Ma	Mc	Mc	Mc
Sc							Sc	Mc	Mc
Ic								Ic	Mc
Mc									Mc

e.g. intermodal coagulation:

$$Ca_{0,ij} = \int_0^\infty \int_0^\infty \beta(d_1, d_2) n_i(d_1) n_j(d_2) dd_1 dd_2$$

Coagulation

free molecular regime:



$$\begin{aligned}
 Ca_{0,ij}^{\text{fm}} &= \int_0^\infty \int_0^\infty \beta_{\text{fm}}(d_1, d_2) n_i(d_1) n_j(d_2) dd_1 dd_2 \\
 &= M_{0,i} M_{0,j} K_{\text{fm}} b_0^{(1)} \left[\sqrt{d_{gi}} \left[e^{\frac{1}{8} \ln^2(\sigma_{gi})} + \sqrt{\frac{d_{gj}}{d_{gi}}} e^{\frac{1}{8} \ln^2(\sigma_{gj})} \right. \right. \\
 &\quad \left. \left. + 2 \frac{d_{gj}}{d_{gi}} e^{\frac{1}{8} \ln^2(\sigma_{gi})} e^{\frac{4}{8} \ln^2(\sigma_{gj})} + \frac{d_{gj}^2}{d_{gi}^2} e^{\frac{9}{8} \ln^2(\sigma_{gi})} e^{\frac{16}{8} \ln^2(\sigma_{gj})} \right. \right. \\
 &\quad \left. \left. + \left(\sqrt{\frac{d_{gi}}{d_{gj}}} \right)^3 e^{\frac{16}{8} \ln^2(\sigma_{gi})} e^{\frac{9}{8} \ln^2(\sigma_{gj})} + 2 \sqrt{\frac{d_{gi}}{d_{gj}}} e^{\frac{4}{8} \ln^2(\sigma_{gi})} e^{\frac{1}{8} \ln^2(\sigma_{gj})} \right] \right]
 \end{aligned}$$

$$\frac{\partial C_{SO_4,l}}{\partial t} = \frac{\pi}{6} \cdot G_l^3 \cdot C_{H_2SO_4}(t)$$

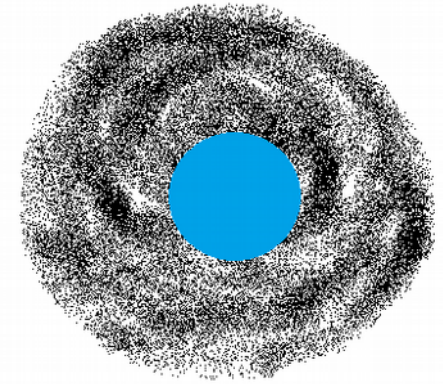
$$G_l^3 = \frac{G_{l,fm}^3 \cdot G_{l,nc}^3}{G_{l,fm}^3 + G_{l,nc}^3}$$

$$G_{l,fm}^3 = \frac{6}{\pi} \frac{\pi \alpha \bar{c}}{4} M_l^2$$

$$G_{l,nc}^3 = \frac{6}{\pi} 2\pi D_v M_l^1$$

Coagulation

near continuum regime:



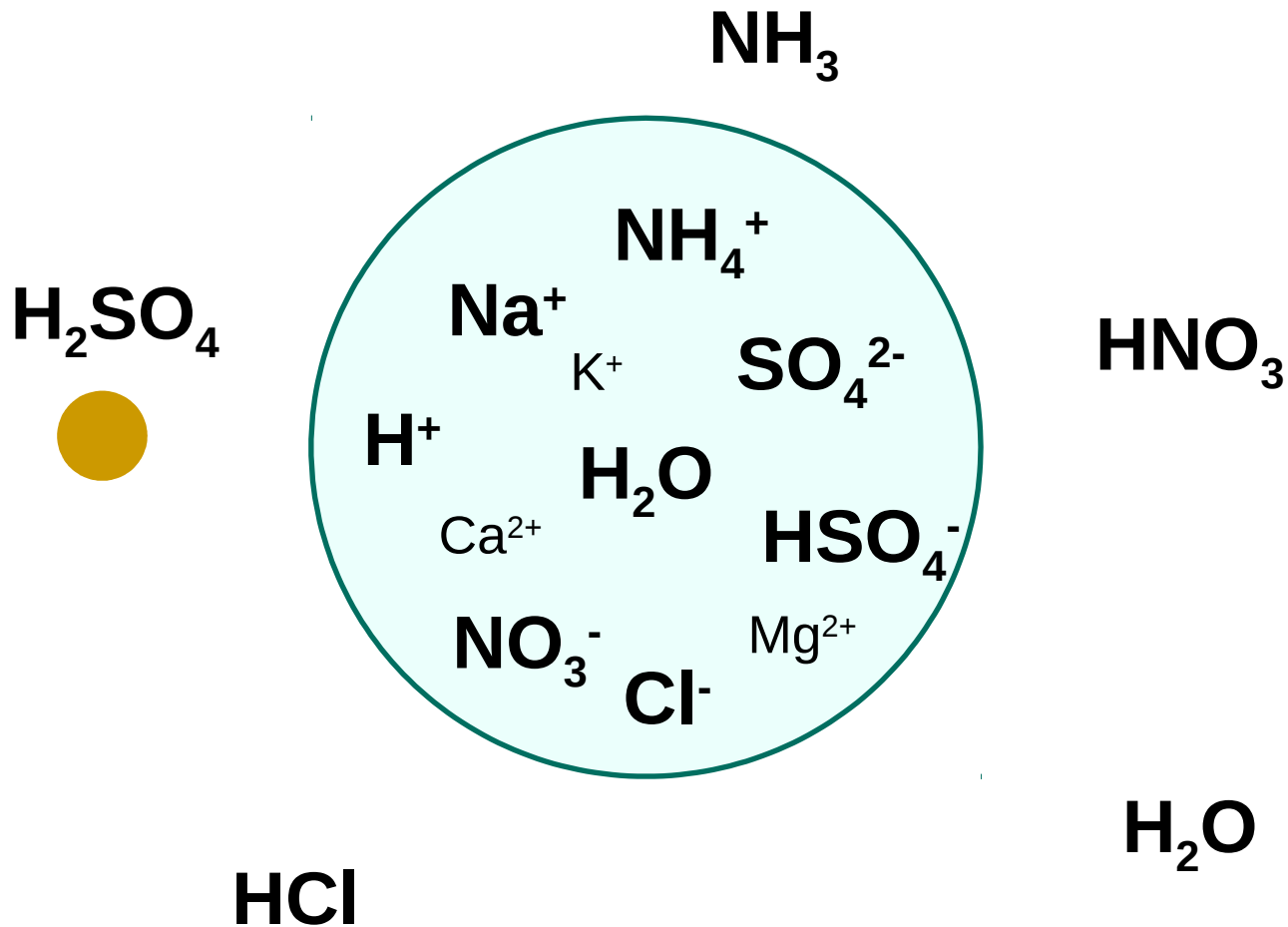
$$\begin{aligned}
 Ca_{0,ij}^{\text{nc}} &= \int_0^\infty \int_0^\infty \beta_{\text{nc}}(d_1, d_2) n_i(d_1) n_j(d_2) dd_1 dd_2 \\
 &= M_{0,i} M_{0,j} K_{\text{nc}} \left[2 + A_i \text{Kn}_{g_i} \left(e^{\frac{4}{8} \ln^2(\sigma_{g_i})} + \frac{d_{g_j}}{d_{g_i}} e^{\frac{16}{8} \ln^2(\sigma_{g_i})} e^{\frac{4}{8} \ln^2(\sigma_{g_j})} \right) \right. \\
 &\quad \left. + A_j \text{Kn}_{g_j} \left(e^{\frac{4}{8} \ln^2(\sigma_{g_j})} + \frac{d_{g_i}}{d_{g_j}} e^{\frac{16}{8} \ln^2(\sigma_{g_j})} e^{\frac{4}{8} \ln^2(\sigma_{g_i})} \right) \right. \\
 &\quad \left. + \left(\frac{d_{g_i}}{d_{g_j}} + \frac{d_{g_j}}{d_{g_i}} \right) \left(e^{\frac{4}{8} \ln^2(\sigma_{g_j})} \right) \left(e^{\frac{4}{8} \ln^2(\sigma_{g_i})} \right) \right]
 \end{aligned}$$

- Calculation of the loss of sulfuric acid on already existing particles
- Calculation of a critical concentration according to Wexler (1994).

$$c_{crit} = 0.16 \cdot \exp\left[0.1 \cdot T - 3.5 \frac{RH}{100} - 27.7\right]$$

- Remaining mass above c_{crit} nucleates and forms new particles

Gas-aerosol partitioning



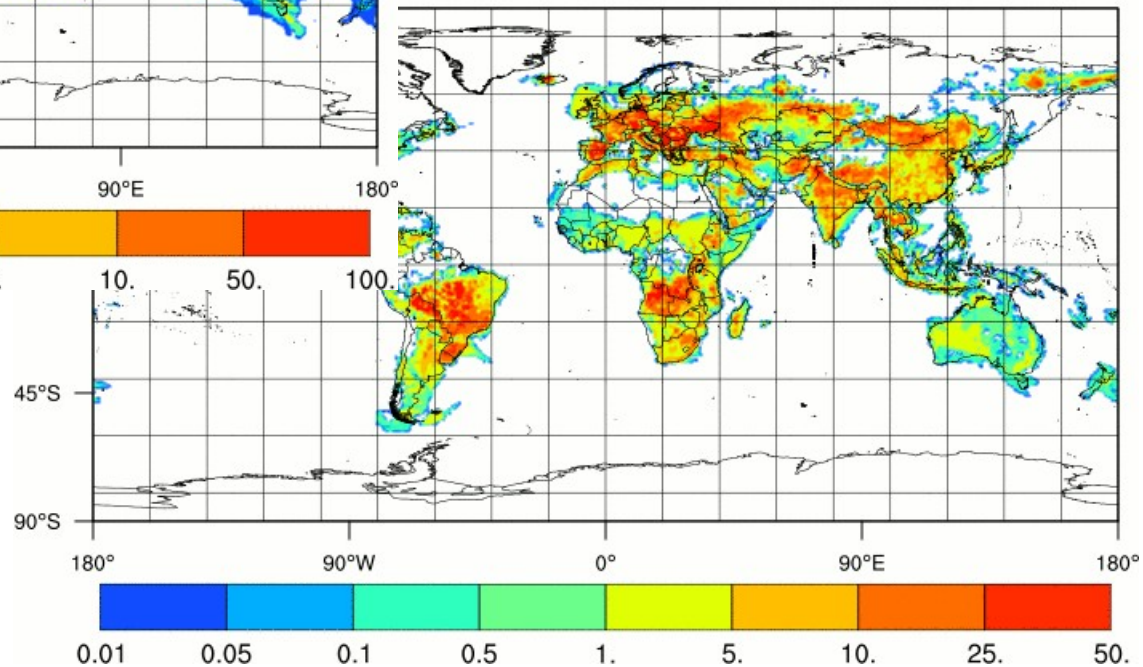
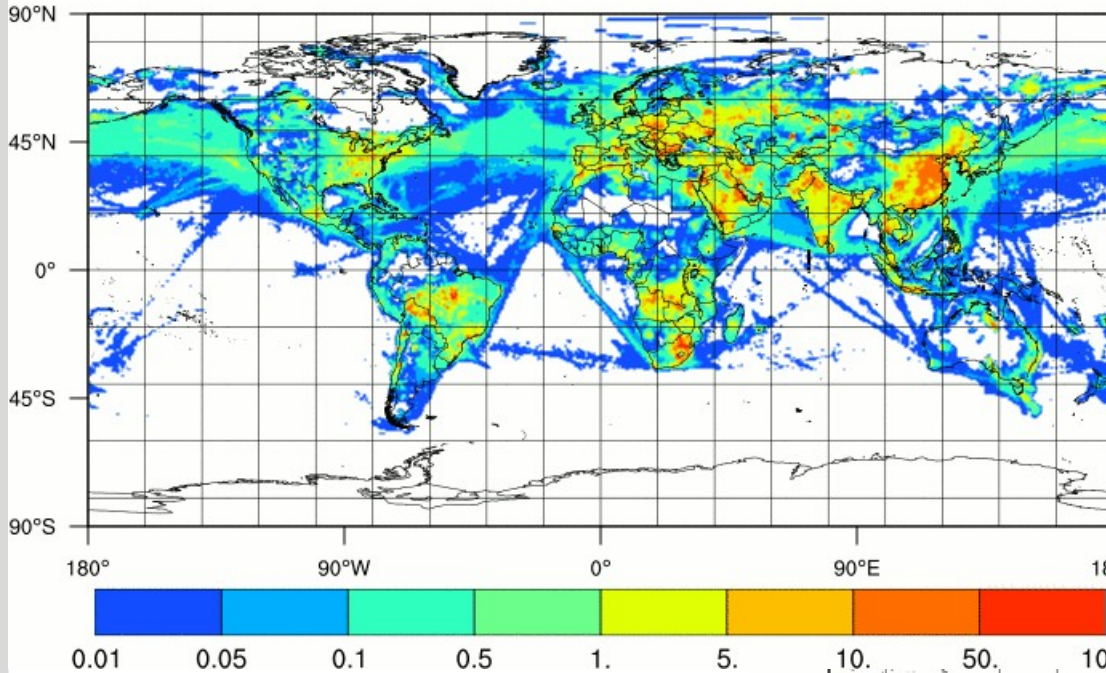
ISORROPIA, Nenes, Fountoukis

Simulated SO₂ and NH₃ concentration

22.7.2017 00 UTC , lvl 89

SO₂(gas) in ppb

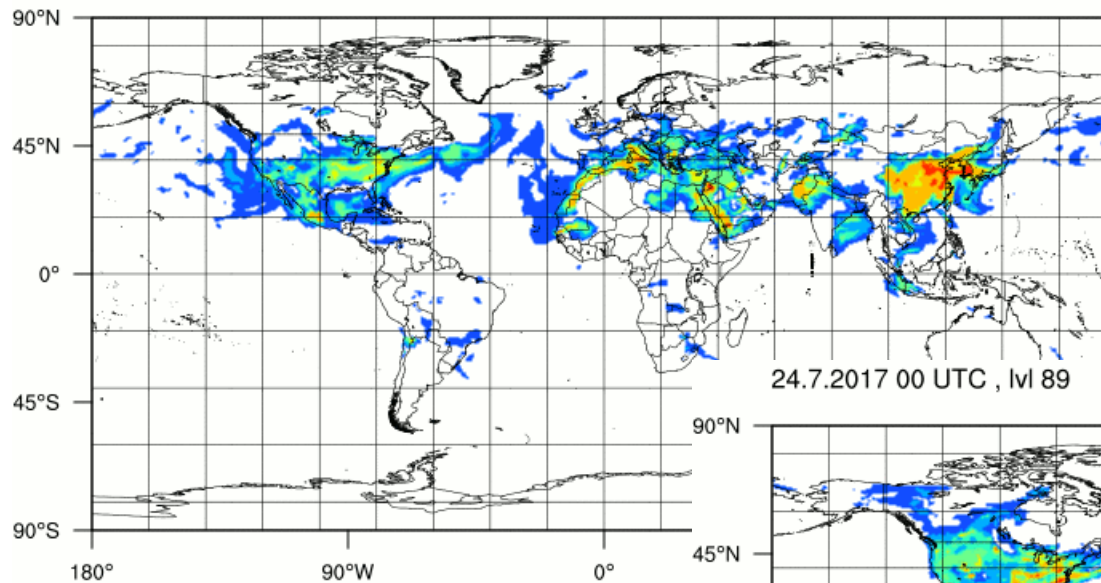
NH₃(gas) in ppb



Sulfate and ammonia concentration

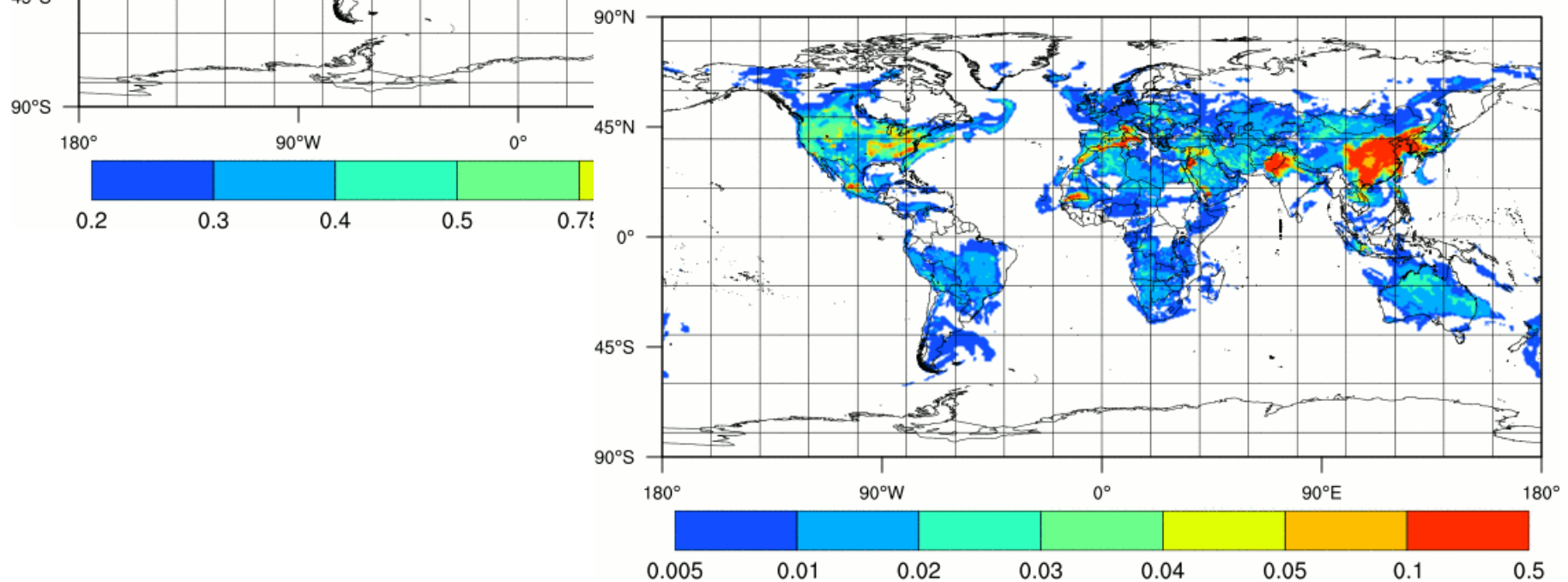
24.7.2017 00 UTC , Ivl 89

SO₄(acc) in $\mu\text{g kg}^{-3}$

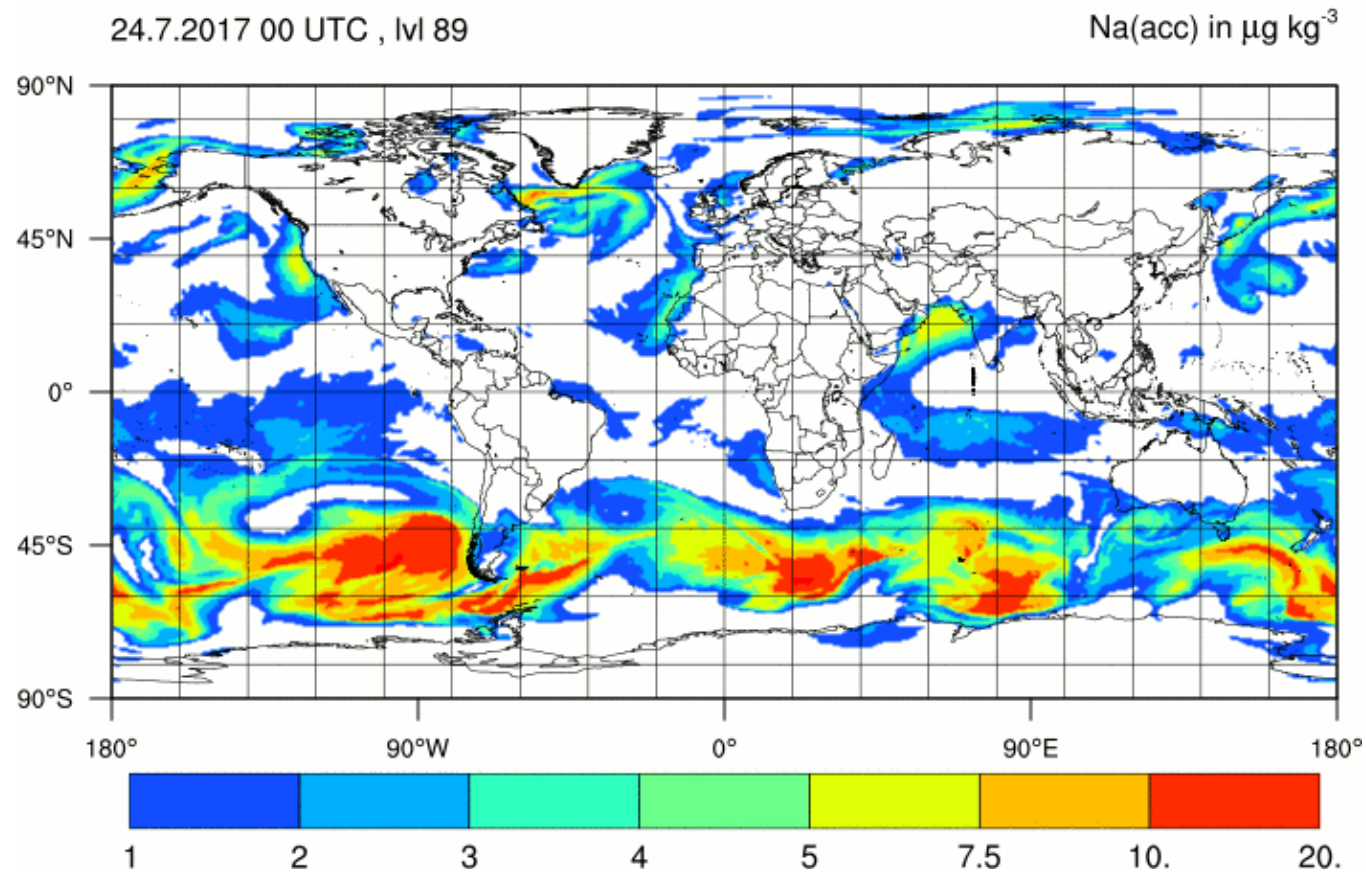


24.7.2017 00 UTC , Ivl 89

NH₄(ait) in $\mu\text{g kg}^{-3}$




Sea salt concentration

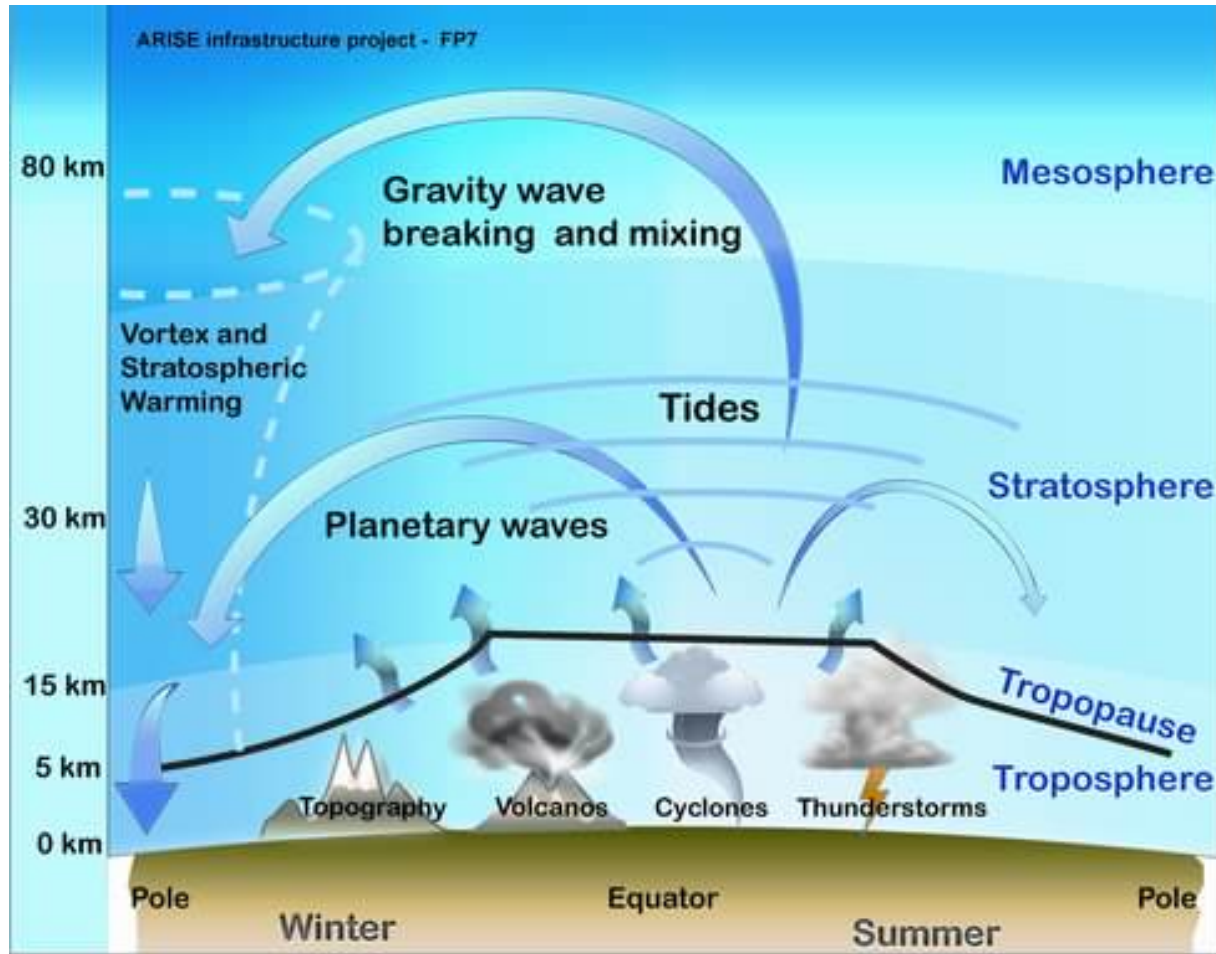


 **New aerosol module for ICON-ART developed and realized (testing phase)**

 **Mode structure allows large range of complexity:**

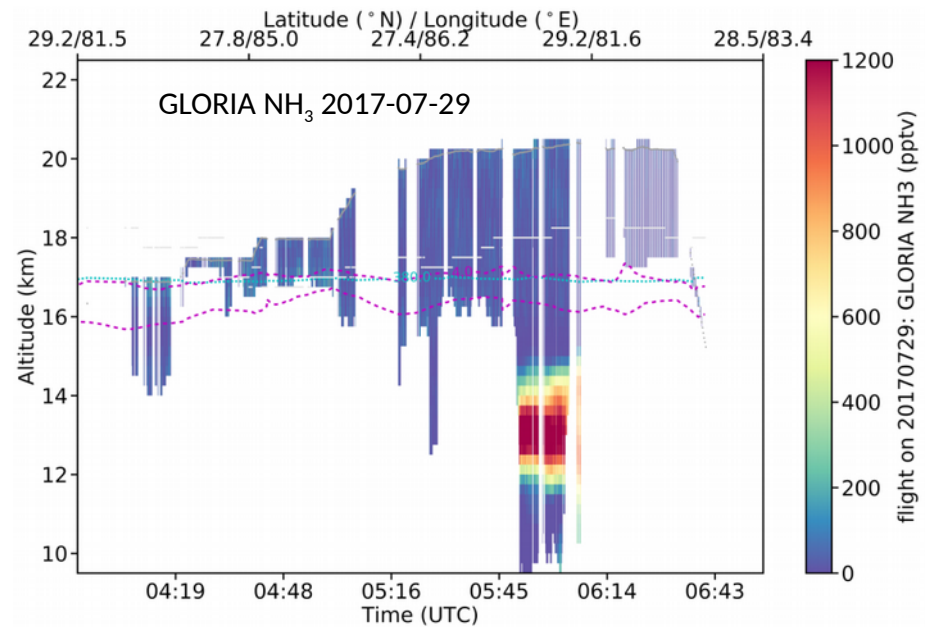
 **reduced aerosol module for NWP-applications**
detailed aerosol module for research

Seamless in the vertical direction



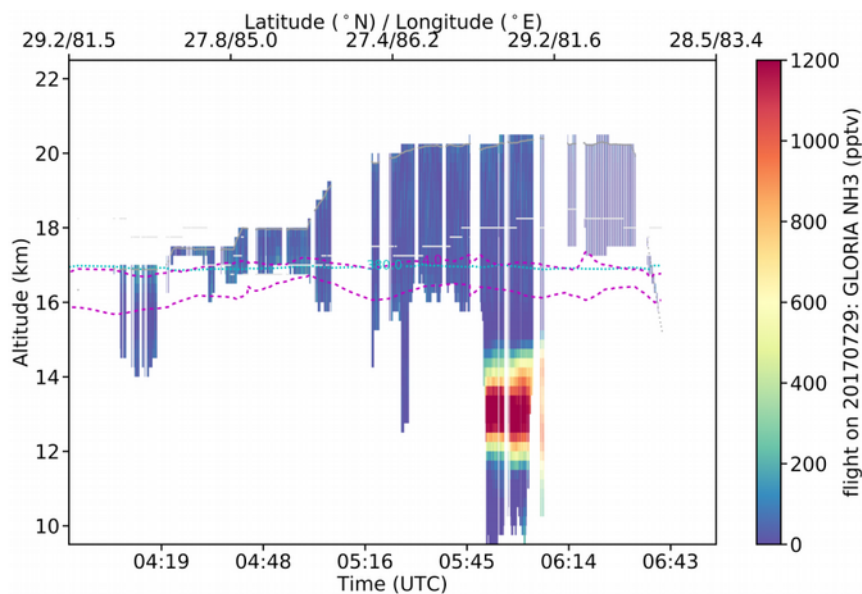
Observations in the Asian Monsoon July 2017

- Very high values (> 1 ppbv) of NH_3 measured (12 km - 14 km)
- ~40 times higher than maximum NH_3 values measured by MIPAS-Envisat
- Inhomogeneous horizontal distribution

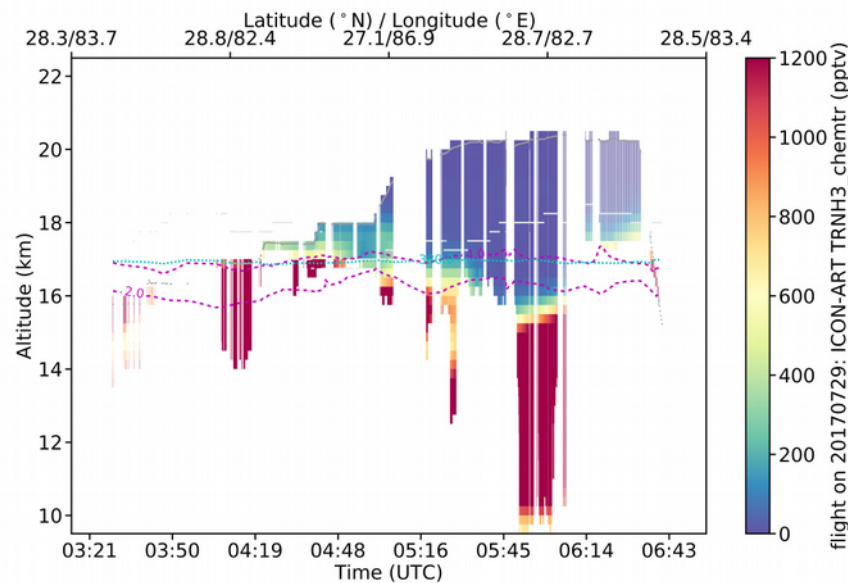


Sören Johansson for the GLORIA Team

GLORIA NH₃ 2017-07-29



ICON-ART NH₃ 2017-07-29



Sören Johannson & Michael Höpfner

Poster: Carmen Ullwer et al., Investigation of the distribution of aerosol-forming trace gases in the UTLS region with ICON-ART



Bernhard Vogel¹
Peter Braesicke²
Ingeborg Bischoff-Gauss⁴
Christopher Diekmann²
Johannes Eckstein²
Jochen Förstner³
Philipp Gasch¹
Tobias Göcke³
Simon Gruber¹
Daniel Rieger^{1,3}
Roland Ruhnke²
Andrea Steiner³
Jennifer Schröter²
Jonas Straub¹
Heike Vogel¹
Carolin Walter¹
Vanessa Bachmann³
Michael Weimer⁴
Sven Werchner¹

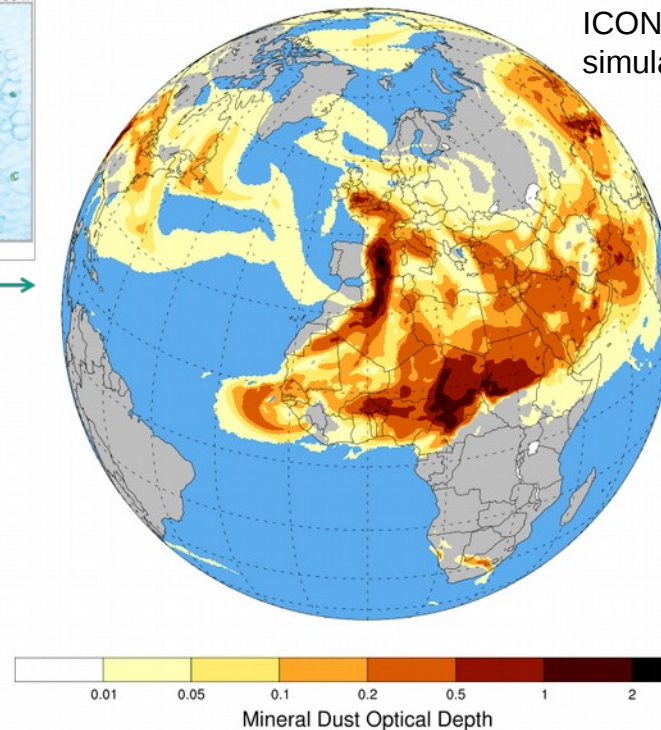
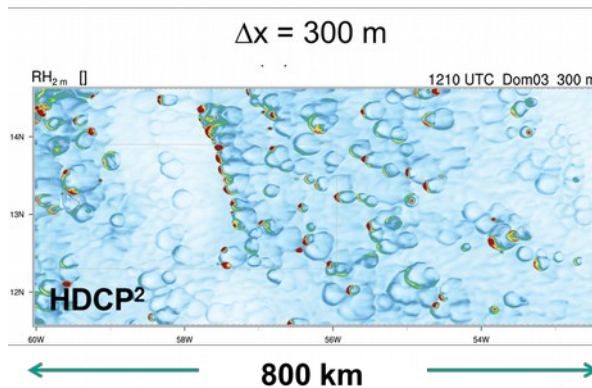
Marco Giorgetta
Hauke Schmidt
Sebastian Rast



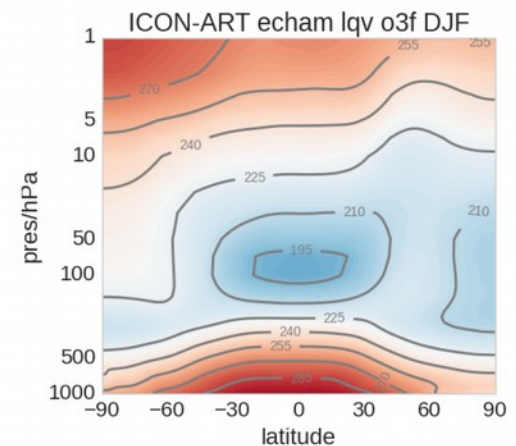
¹ KIT, Institute of Meteorology and Climate Research – Troposphere Research
² KIT, Institute of Meteorology and Climate Research – Atmospheric Trace Gases and Remote Sensing
³ Deutscher Wetterdienst (DWD)
⁴ KIT, Steinbuch Centre for Computing

What makes ICON and ICON-ART unique?

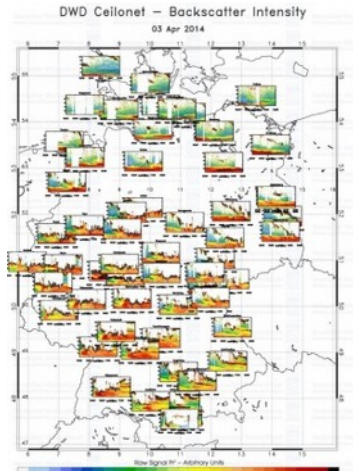
- Seamless in horizontal and vertical scales (troposphere-mesosphere)
- Seamless in time (seconds-decades): (LES) – Weather – Climate



ICON (Climate) temperature structure with interactive ozone



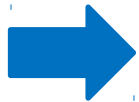
Link between observation and simulation



Attenuated
backscatter

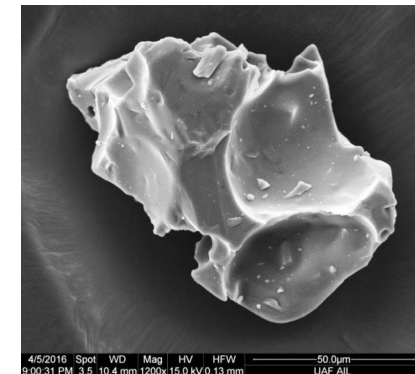
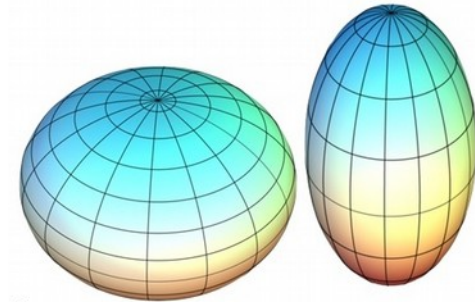
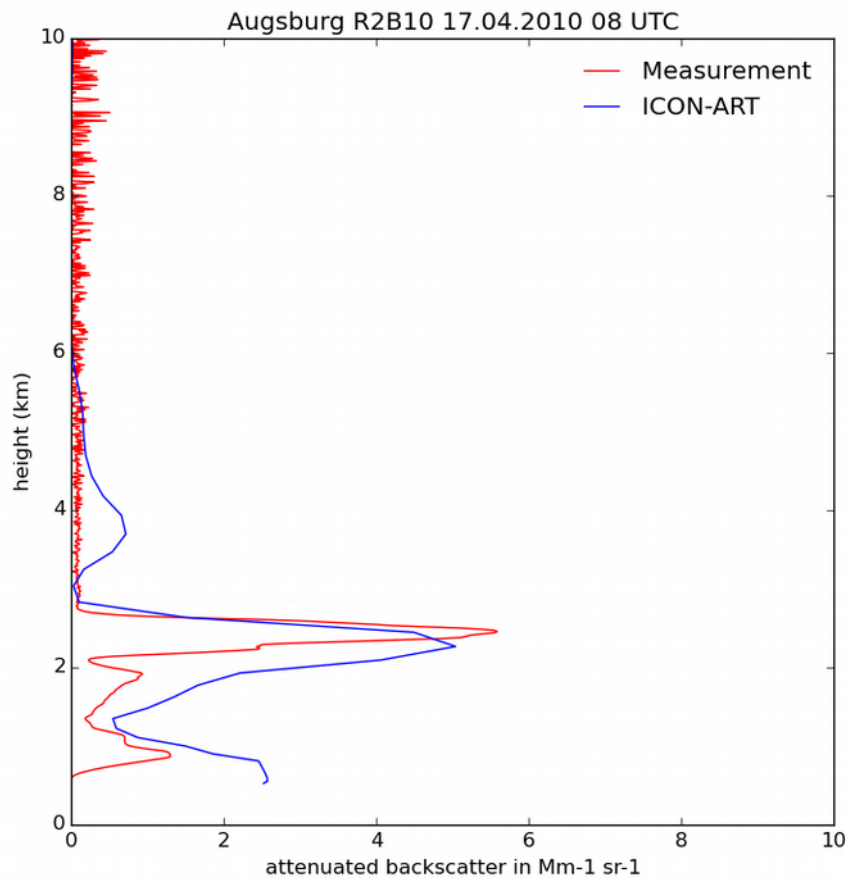


Aerosol
concentration



Development and implementation of forward operators of natural and anthropogenic aerosol

Vertical profile of attenuated backscatter



Link between observation and simulation



Attenuated
backscatter



Aerosol
concentration



$$P(z) = C_L \frac{\beta(z)}{z^2} \exp\left(-2 \int_0^z \alpha(z') dz'\right)$$

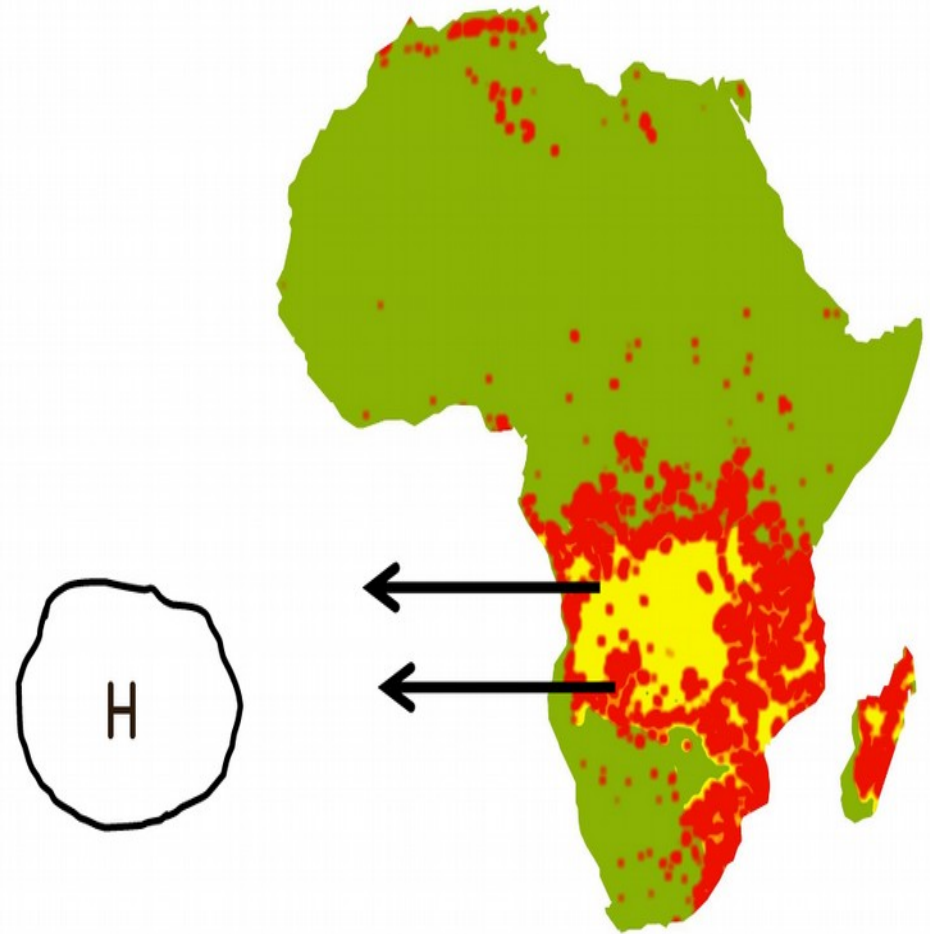
Frequently the Lidar ratio S is used to derive the backscatter coefficient

$$\beta(\lambda) = \frac{\alpha(\lambda)}{S}$$



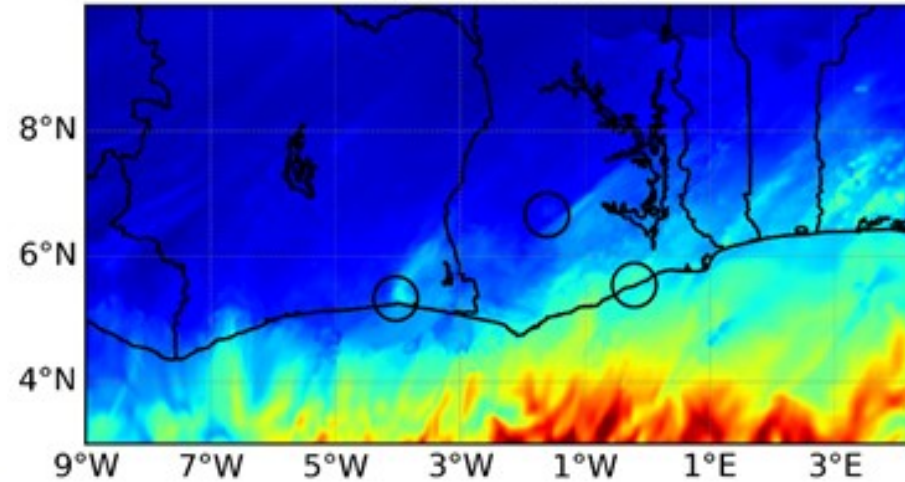
Preferable: Direct calculation of the backscatter coefficient

- Evidence of biomass burning plumes in central and south Africa from June to September.
- According to Mari et al, 2008, there is a long-range biomass transport which is carried Westward by a jet at 700 hPa between 2 to 4 km
- High-pressure region to the West of African continent might play a role to mix it into the boundary layer. (Haslett, 2017)

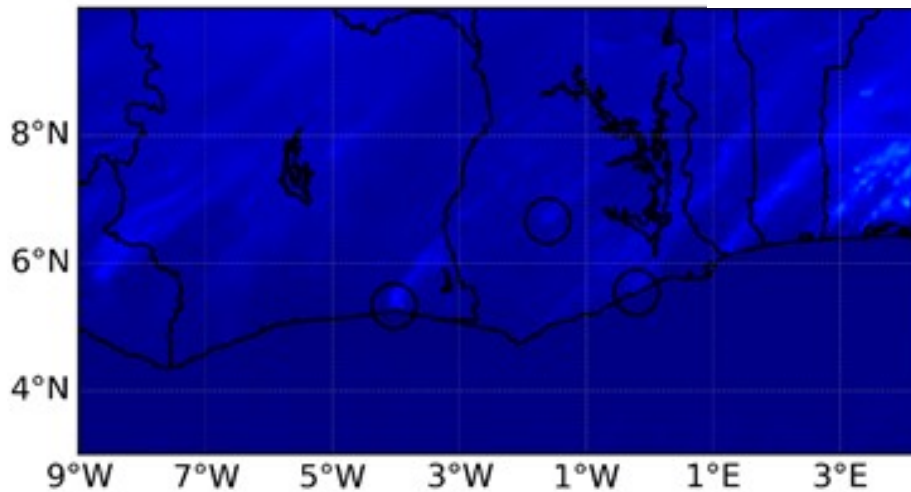


Organic aerosol wo/w vegetation fire

FIRE at 12 UTC

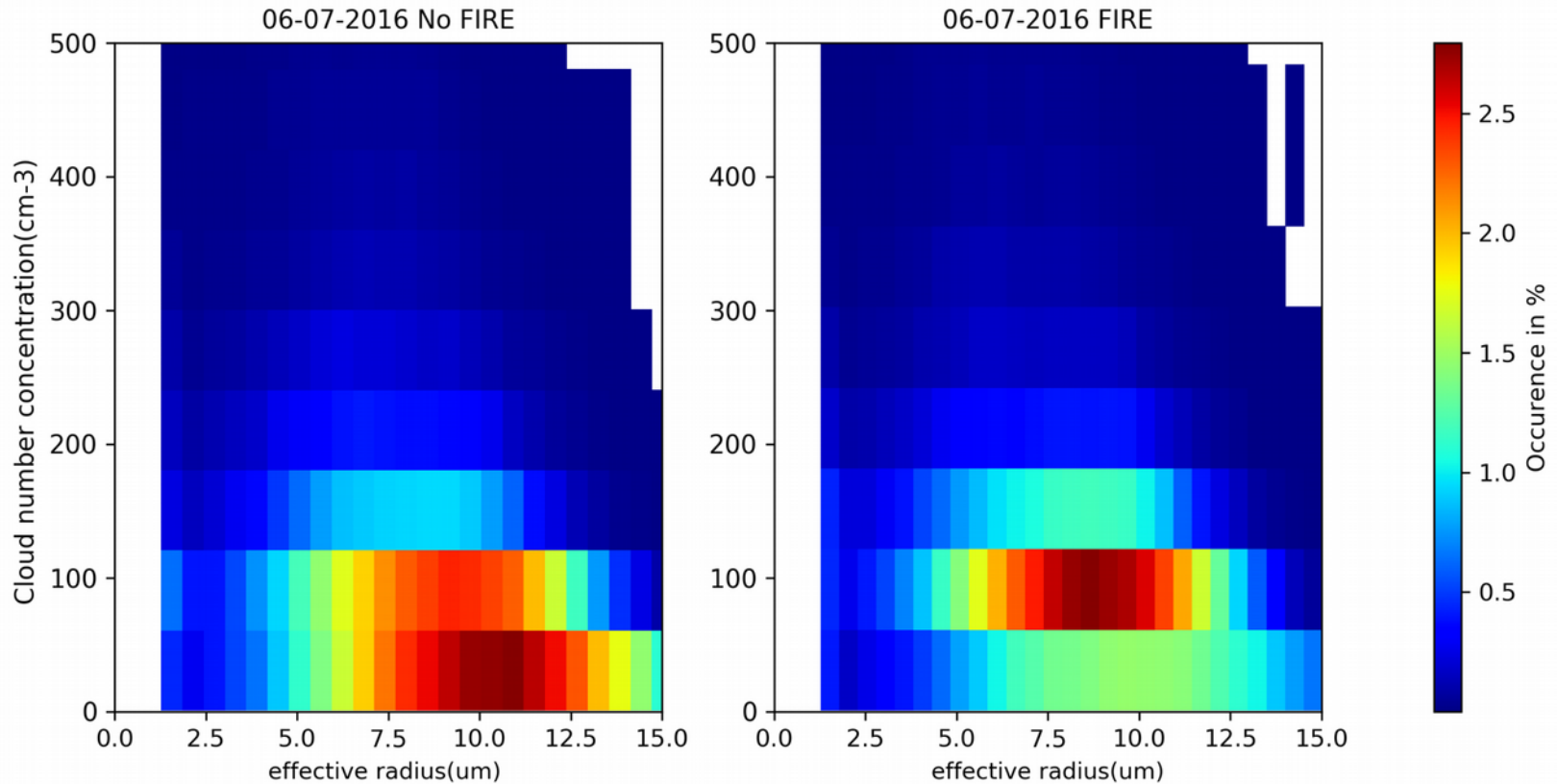


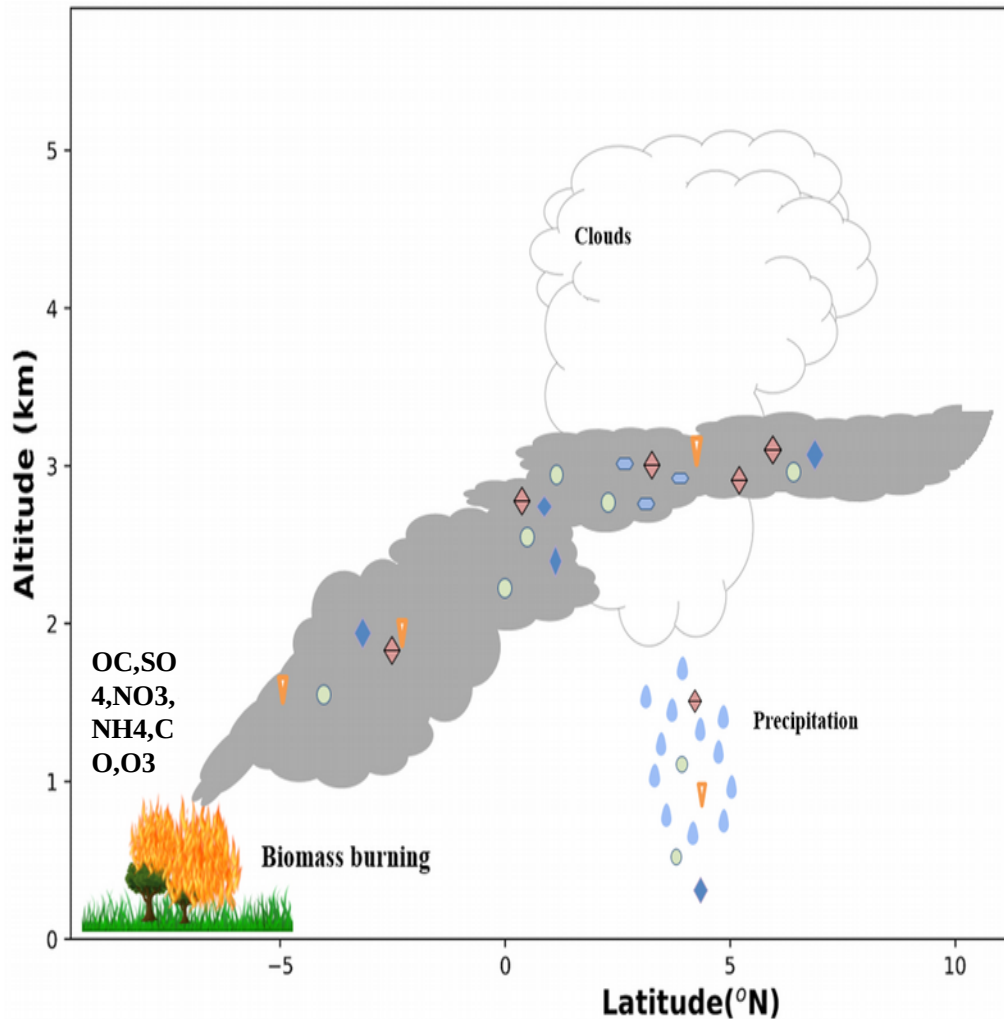
NO FIRE at 12 UTC



Impact on CDN and r_e

Joint histogram for domain 9W-4.33E, 3N-10N

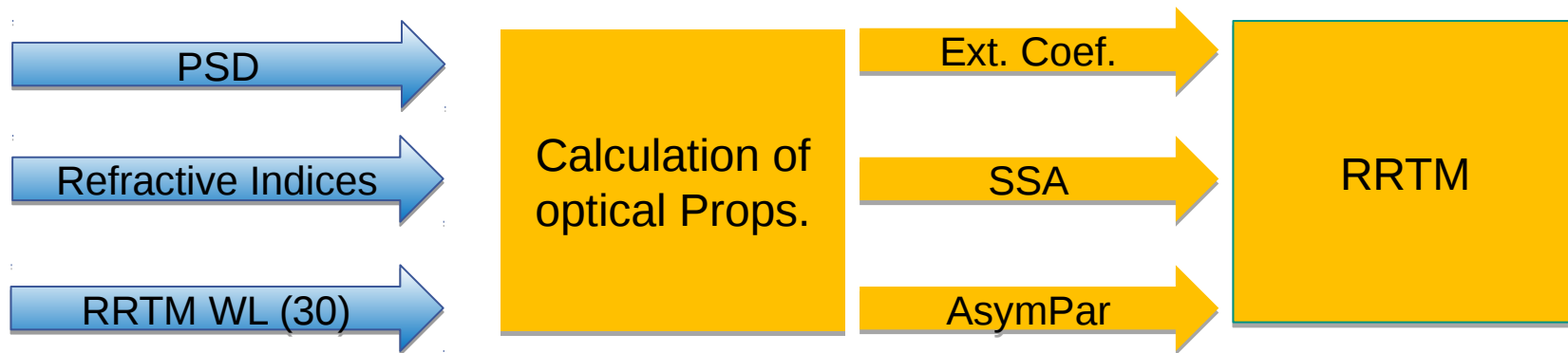




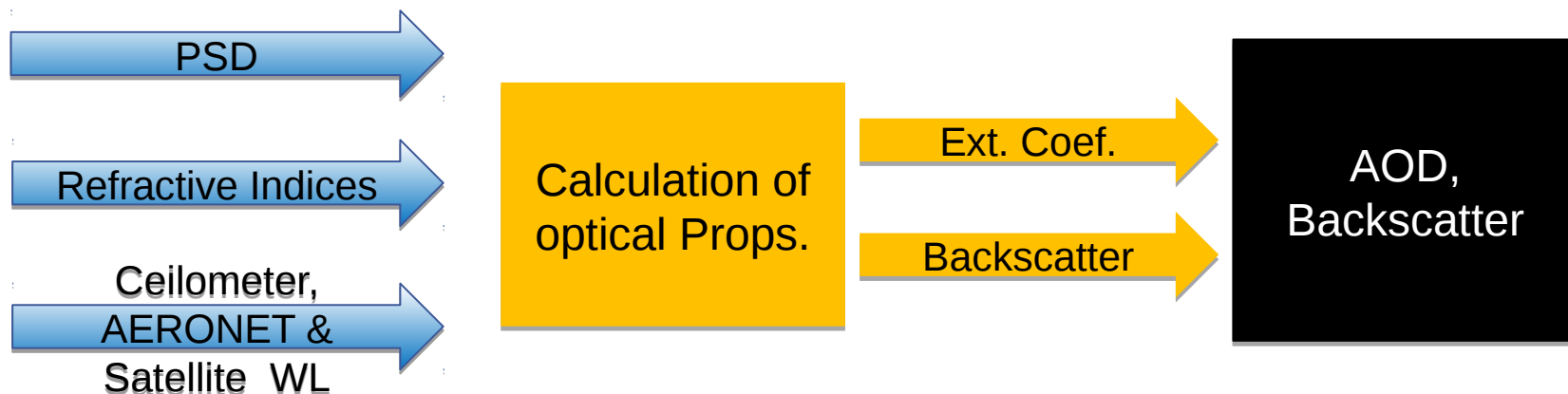
- ☁️ **Clouds** bring aerosols from aloft into PBL.
- ☁️ **7.46%** increase of CDNC over the DACCIWA region and **32.92%** over the marine domain.
- ☁️ **50 w/m²** decrease in direct surface incoming SW radiation
- ☁️ Mass concentration flux rate can reach **5 $\mu\text{g m}^{-2} \text{s}^{-1}$** .

Dust optical properties in ICON-ART

Prognostic (for direct radiative effect):

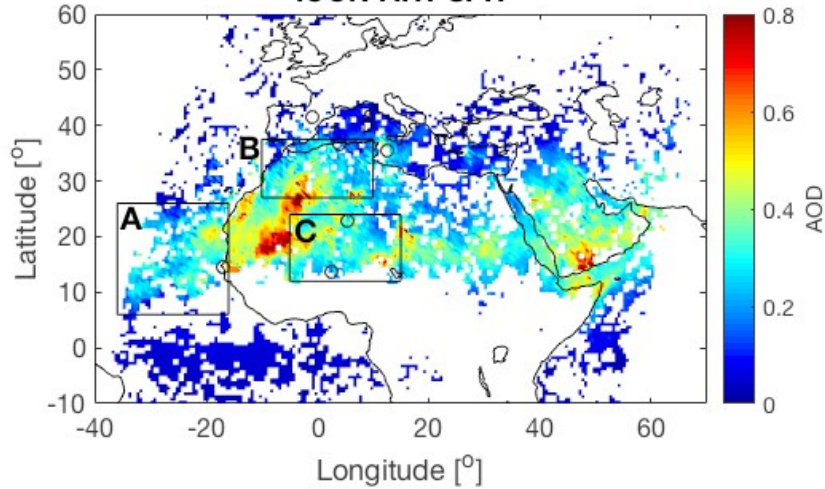


Diagnostics (for AOD and AB):

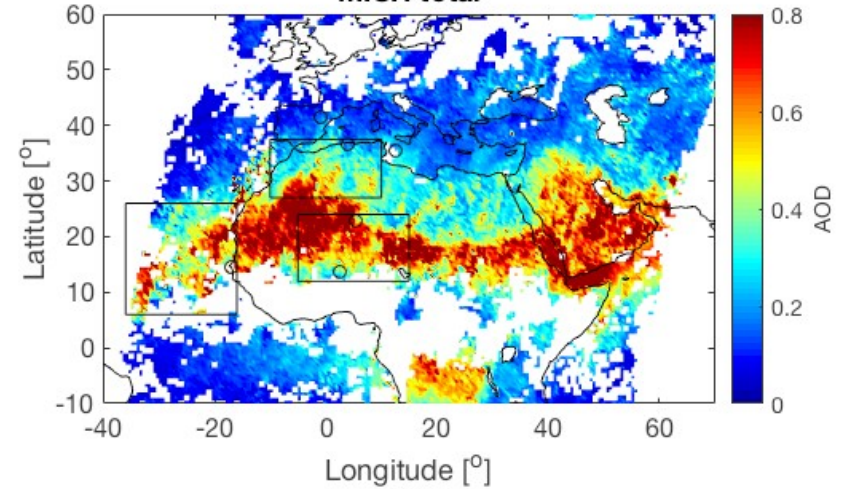


Verification: Mean AOD July 2017

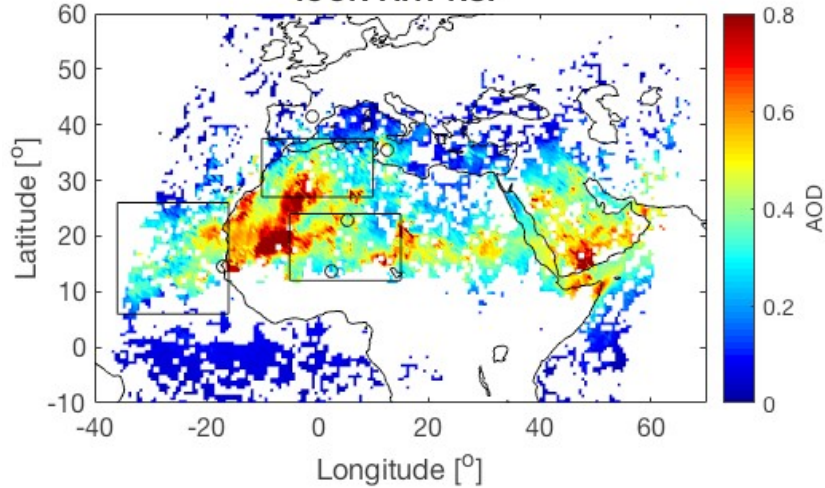
ICON-ART SPH



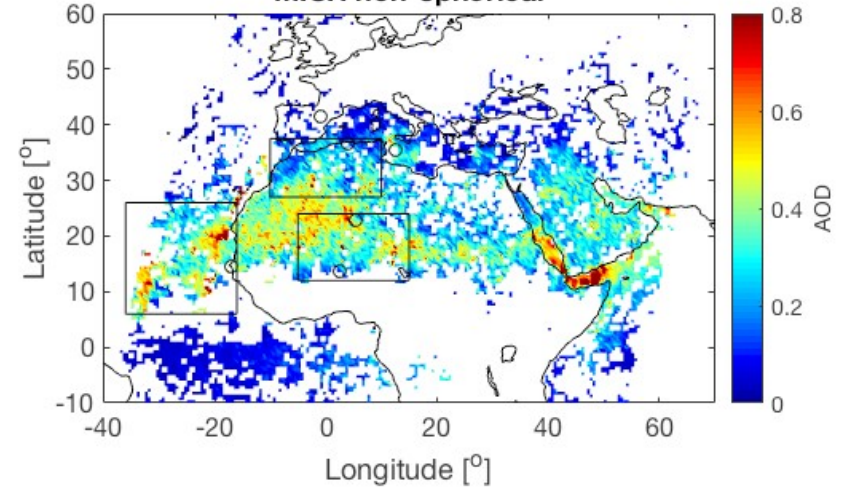
MISR total



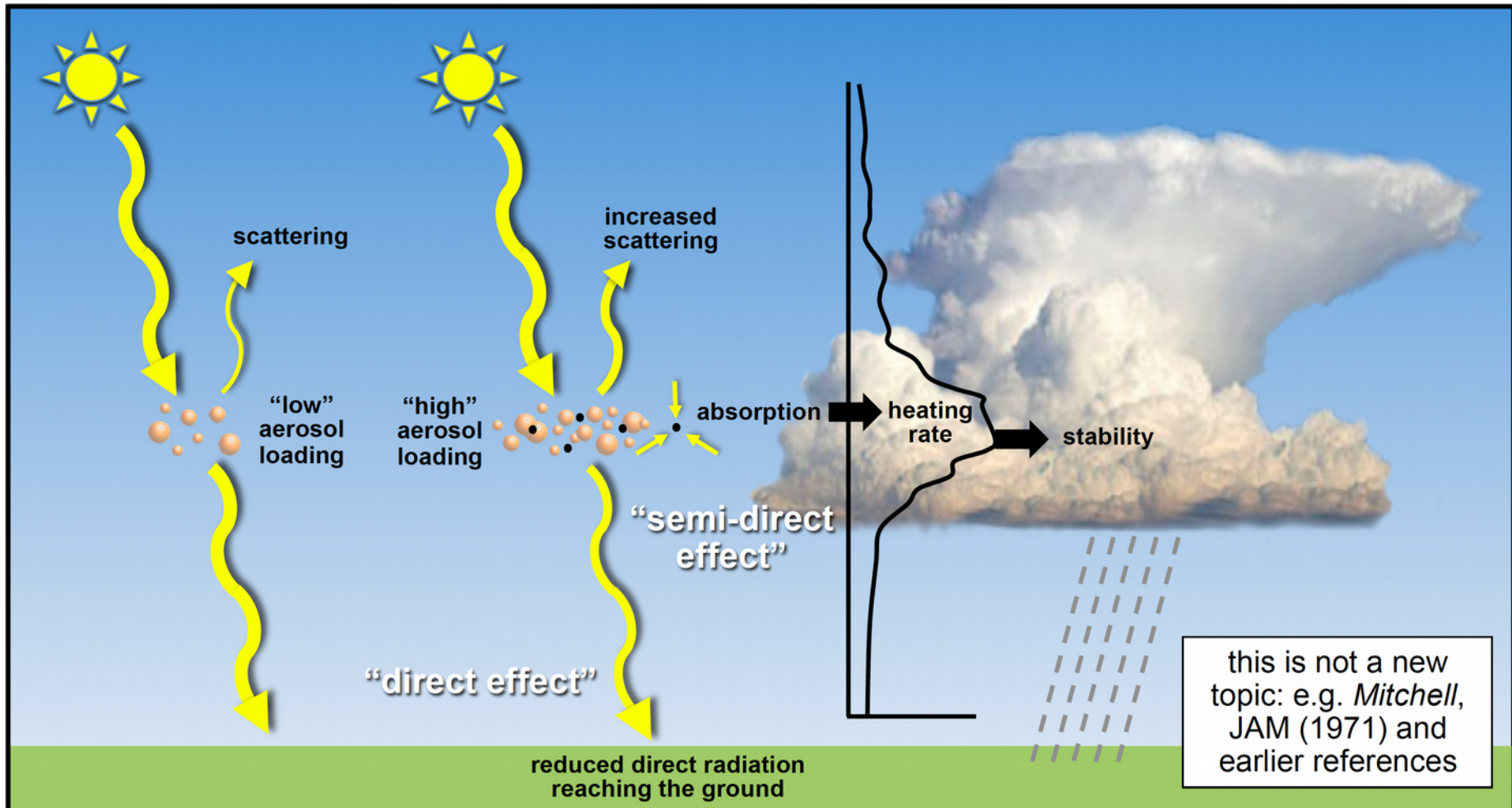
ICON-ART NSP



MISR non-spherical



Impact of particles on radiation



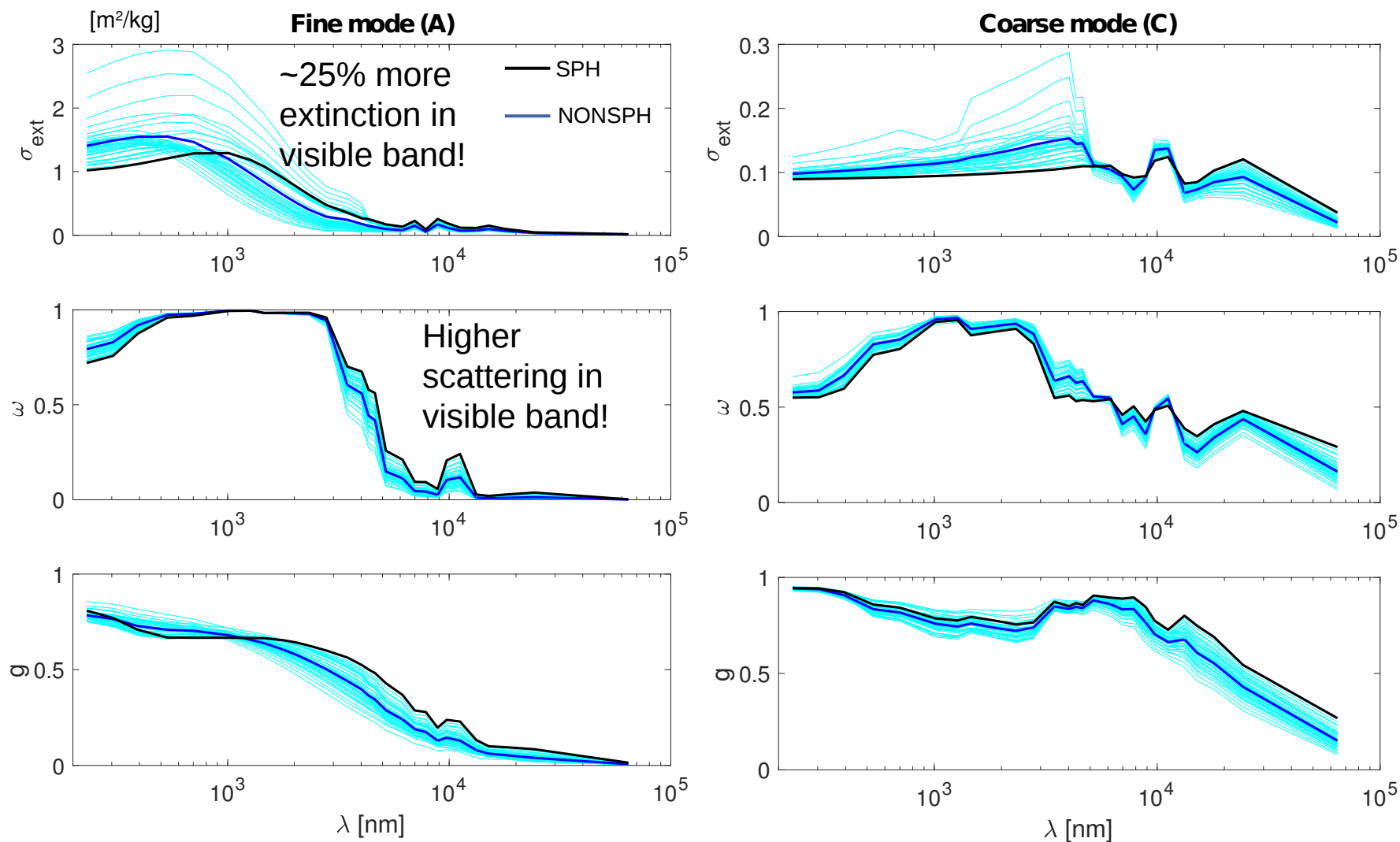
Photovoltaic Energy Generation



Surface heat and latent heat fluxes

Source: Alma Hodzic, NCAR

Calculated optical properties



- Particle size distribution (emitted and transported)
- Variable median diameter and its impacts on optical props
- Dynamic land surface properties for emissions
- Parameterization of convective dust emission

Hoshyaripour, G., Bachmann, V., Förstner, J., Steiner, A., Vogel, H., Wagner, F., Vogel, B.
Accounting for Particle Non-sphericity in a Dust Forecast System: Impacts on Model-
Observation Comparison, submitted to JGR

- 🌤️ Operational pollen forecast at MeteoSwiss (web page and app!)
- 🌤️ Simulation of air quality in the area of Karlsruhe and comparison with detailed measurements (IMK-AAF)
- 🌤️ EMPA
- 🌤️ Investigation of timestep dependency of aerosol-cloud-convection modelling study results:
Barrett et al 2018: "One Step at a Time: How Model Timestep Significantly Affects Convection-Permitting Simulations"
submitted to Journal of Advances in Modelling Earth Systems (JAMES)